Tampere University

Sofia Ylihärsilä

ASTROCYTIC GLUTAMATE TRANSPORTERS: PHYSIOLOGY AND SIMULATIONS

Faculty of Medicine and Health Technology
Master's thesis
May 2023

ABSTRACT

Sofia Ylihärsilä: Astrocytic Glutamate Transporters: Physiology and Simulations
Master's thesis
Tampere University
Master's Programme in Biotechnology and Biomedical Engineering
Supervisors: Marja-Leena Linne and Tiina Manninen
Examiners: Marja-Leena Linne and Matti Nykter
May 2023

Astrocytes have many roles in the central nervous system, ranging from homeostatic regulation to information processing in the brain. One function of astrocytes is the uptake of glutamate from the synaptic cleft using glutamate transporters (excitatory amino acid transporters). The uptake of glutamate is a critical process, which enables correct neurotransmission and prevents excitotoxicity and neurodegenerative conditions.

In this work, the goal was to study glutamate transporters in detail using a computational single-cell astrocyte model. A six-state cyclic kinetic scheme of the transporter, with reversible reactions and realistic kinetic constants, was incorporated into ASTRO simulation environment. In addition to the transporter properties, the possible association of a calcium signal with the glutamate transport process was studied by adding a sodium-calcium exchanger model which was available in ModelDB database.

In the simulations, an increased glutamate concentration in the extracellular space activates the glutamate transporters. The response of the model is examined in terms of concentration changes of different ions and current amplitudes and durations. The simulations showed a fast uptake of extracellular glutamate, which in the case of 0.5 mM extracellular glutamate occurred in 5 ms. The current generated by the transporter was measured in a voltage clamp simulation of ASTRO tool, which showed an amplitude of 0.25 nA and a duration of about 50 ms. Regarding the calcium signal, the sodium-calcium exchanger was found to reverse its function and thus transport calcium into the cell when glutamate transporters were active, creating a detectable calcium signal. However, the physiological relevance of this signal is not yet known, and more studies are needed to address this question.

The response of the model to different extracellular glutamate concentrations was also studied, and the result was that doubling the glutamate concentration increased the uptake time by 700%. Furthermore, the model was sensitive to different transporter amounts. A 30% reduction in transporter amount led to glutamate uptake time increasing by 300%. This would be an interesting research question for experimental studies, because transporter trafficking to the membrane could be one mechanism that gets disturbed in brain disorders and diseases, leading to decreased transporter amounts, and resulting in excess glutamate at the synaptic cleft.

Keywords: astrocyte, excitatory amino acid transporter, calcium signal, computational model, glutamate transporter, sodium-calcium exchanger

PREFACE

This thesis was done in Computational Neuroscience group at Tampere University. The supervisors were Group Leader, Senior Research Fellow Marja-Leena Linne and Academy Research Fellow Tiina Manninen. I want to thank Marja-Leena for the opportunity to do this thesis in her group and both Marja-Leena and Tiina for all the feedback and comments. I would also like to thank other members of the group, especially Saana Seppälä for peer support and discussions.

Tampere, 15 May 2023

Sofia Ylihärsilä

CONTENTS

LIST OF FIGURES

LIST OF SYMBOLS AND ABBREVIATIONS

Biological abbreviations

5-HT_{1A}, 5-HT_{2A}, 5-HT_{2B}, 5-HT_4, 5-HT_{5A}, 5-HT_7	Serotonin receptors
Aβ	Amyloid beta
A_1, A_2, A_3	Adenosine receptors
ABCA1	ATP-binding cassette transporter A1
Acs-1	Cationic amino acid transporter
AD	Alzheimer's disease
ANLS	Astrocyte neuron lactate shuttle
AQP4a, AQP4c, AQP4e	Aquaporin isoforms
ASCT2	Neutral amino acid transporter subtype
AT_1, AT_2	Angiotensin receptors
ATP	Adenosine triphosphate
B0,+	Neutral and basic amino acid transporter
BK/K_{Ca}1.1	Large-conductance Ca^{2+}-activated K^+ channel
C5L2	Complement 5a-like receptor
Ca^{2+}	Calcium ion
CAAC	Ca^{2+}-activated Cl^- channel
CaSR	Ca^{2+}-sensing receptor
Ca_v	Voltage-gated Ca^{2+} channel
CB_1	Cannabinoid receptor
CB-like	Cannabinoid-like
CICR	Ca^{2+}-induced Ca^{2+} release
Cl^-	Chloride ion
ClC	Voltage-gated anion channel
CNG	Cyclic nucleotide gated channel
CTL1	Choline transporter-like protein 1
CXCR2, CXCR4, CCR1, CCR2, CCR3, CCR5, CCR10, CCR11, CX3CR1	Chemokine receptors
CysLT1, CysLT2	Cysteinyl leukotrienes receptors
D_1, D_2, D_3, D_4	Dopamine receptors
DAT1	Na^+-dependent dopamine transporter
EAAT	Excitatory amino acid transporter
EGFR	Epidermal growth factor receptor
EP3	Prostaglandin E receptor 3
Eph	Ephrin
ER	Endoplasmic reticulum
ER-α	Estrogen receptor α
FGFR1	Fibroblast growth factor receptor 1
FRAP	Fluorescence recovery after photobleaching
GAT	GABA transporter
GFAP	Glial fibrillary acidic protein
GLP-1R	Glucagon-like peptide-1 receptor
GLT-1	Glutamate transporter 1
Glu^-	Glutamate
GluR5-GluR7, KA1, KA2	Kainate receptors
GlyT	Glycine transporter
GPCR	G-protein coupled receptor

GPER-/GPR-30	G-protein coupled estrogen receptor
GPR37L1	G-protein coupled receptor GPR37-like 1
H^+	Hydrogen ion
HCAR1	Hydroxycarboxylic acid receptor 1
HCO_3^-	Bicarbonate
IFN-γ	Interferon-γ
IGF-1	Insulin-like growth factor 1
iGluSnFr	Glutamate-sensitive fluorescent reporter
IJ_1AR, IJ_2AR, b_1AR, b_2AR	Adrenergic receptors
IL-1β	Interleukin-1β
ILR1	Interleukin-1 receptor 1
$[ion]_{in}$	Intracellular concentration of an ion
$[ion]_{out}$	Extracellular concentration of an ion
IP_3	Inositol-trisphosphate
IP_3R	IP_3 receptor
IP_3R2	IP_3 receptor type 2
IR	Insulin receptor
Jak	Janus kinase
K^+	Potassium ion
K-ATP	ATP-sensitive K^+ channel
KCC	K^+-Cl^- cotransporter
Kidins220	Kinase-D interacting substrate of 220 kDa
K_{ir}	Inwardly rectifying K^+ channel
LepR	Leptin receptor
LPA	Lysophosphatidic acid
LPL	Lipoprotein lipase
LTD	Long-term depression
mChR M_1-M_5	Muscarinic cholinoreceptors
MCT	Monocarboxylate transporter
MEA	Microelectrode array
mGluR	Metabotropic glutamate receptor
mPTP	Mitochondrial permeability transition pore
Na^+	Sodium ion
Na^+/K^+-ATPase	Na^+-K^+ pump
Na_v	Voltage-gated Na^+ channel
NBC	Na^+/HCO_3^- cotransporter
NCCa-ATP	ATP-dependent, nonselective cation channel
NCX	Na^+-Ca^{2+} exchanger
NET	Norepinephrine transporter
NHE	Na^+/H^+ exchanger
NKCC	$Na^+/K^+/Cl^-$ cotransporter
NMDA	N-methyl-D-aspartate
NTSR2	Neurotensin receptor 2
OAP	Orthogonal array of particles
OCTN2	Carnitine transporter
P2X7	P2X purinoceptor 7
PAC_1	PACAP receptor
PAR	Protease-activated receptors
PDGFRα	Platelet-derived growth factor receptor α
PEPT2	H^+-peptide transporter
PMCA	Plasma membrane ATP-driven Ca^{2+} pump
RVD	Regulatory volume decrease
RyR	Ryanodine receptor
S1P	Sphingosine-1-phosphate
SERT	Serotonin transporter

SK/K_{Ca}	Small conductance Ca^{2+} activated K^+ channel
SNAT	Neutral amino acid transporter
SOCC	Store-operated calcium channel
SR-A	Class-A scavenger receptor
Stat	Signal transducer and activator of transcription
STDP	Spike-timing-dependent plasticity
STEPS	Stochastic Engine for Pathway Simulation
SVCT2	Na^+-dependent ascorbic acid transporter
TAAR1	Trace amine-associated receptor type-1
TCA	Tricarboxylic acid
TfR1	Transferrin receptor 1
TGFβ	Transforming growth factor β
TGF-βR	Transforming growth factor β receptor
TLR	Toll-like receptor
TREM-2	Triggering receptor expressed on myeloid cells-2
TrkB	Neurotrophin receptor
TRP	Transient receptor potential channel
VEGF	Vascular endothelial growth factor
VIPR	Vasoactive intestinal polypeptide receptors
VRAC	Volume-regulated anion channel
VSOR	Volume-sensitive outwardly rectifying channel
ZnT	Zink transporter

Modelling-specific symbols

C	Capacitance
C_m	Specific membrane capacitance
d	Diameter
E	Equilibrium potential
E_k	Equilibrium potential for K^+
E_L	Equilibrium potential for leak current
F	Faraday constant
g	Conductance
$\overline{g_L}$	Leak current conductance
I	Current
i_a	Axial current
i_{ion}	Current through membrane
k	Rate constant
K_m	Half saturation constant
$[K^+]_o$	Extracellular K^+ concentration
K_v	Voltage-activated K^+ channels
q	Charge
R	Gas constant / resistance
R_a	Axial resistivity
t	Time
T	Temperature
U	Voltage
V_m	Membrane potential
v_{max}	Maximum uptake rate
x	Distance
z	Number of charges

1. INTRODUCTION

Astrocytes are an important glial cell type of the central nervous system. They make up a large percentage of the cells found in the central nervous system, with estimations varying from 20% to above 50% depending on the species (Hasel and Liddelow, 2021). The functions of astrocytes include for example homeostasis of ions and neurotransmitters, and control of energy metabolism and vascular function (Haim and Rowitch, 2017). However, astrocytes must be seen as a heterogeneous cell type. A recent study found that different astrocyte subtypes exist in a layer structure in the cerebral cortex (Bayraktar et al., 2020). Also, there is evidence of neural circuit-specific astrocytes, which are diverse in their physiological and anatomical properties (Chai et al., 2017).

In addition to experimental studies, astrocyte functions can be studied with computational models. The models can include only astrocytes or astrocytes and neurons, and the models range from single-cell to network models. Some models also include vascular elements. Astrocyte contribution to neural dynamics is being recognized, and in neuronal network models, astrocytes have been added to study for example synchronization of neural activity (Manninen et al., 2023). Many of the astrocyte models that have been developed study calcium (Ca^{2+}) dynamics in astrocytes (Manninen et al., 2018). Recent advancements in astrocyte modelling include recognizing their contribution to higher cognitive functions, for example incorporating astrocytes to models of short-term plasticity (Becker et al., 2022) and long-term plasticity (Manninen et al., 2020).

In this Master's thesis, the goal is to study astrocyte physiology with a single-cell astrocyte model. The specific interest is the function of glutamate transporters called excitatory amino acid transporters (EAATs). Glutamate transporters move glutamate from the synaptic cleft into astrocytes. Glutamate is the main excitatory neurotransmitter in the brain, and glutamate transporters are responsible for clearing the glutamate which is released from neurons. Thus, the transporters enable neurotransmission to function correctly. Glutamate transport can be considered as one of the most important functions of astrocytes. It is also a process, in which the cells invest a lot of energy, and mitochondria have been found to localize near the transporters to generate the needed energy (Jackson et al., 2014). Glutamate transporter dysfunction has been associated with neuronal

excitotoxicity and neurodegeneration, and as an example, in a familial form of Parkinson's disease, transporter dysfunction has been found to be a possible cause of excess glutamate and neurodegeneration (Iovino et al., 2022).

The possible involvement of glutamate transporters in several diseases, including neurodegenerative diseases which are becoming more relevant with aging populations and increased life expectancy, makes them an interesting research topic. Also, their key role in healthy brain function causes interest in the exact mechanisms by which they work, including how fast the process is, and what the physiological consequences are.

Next, Literature Review of the most important physiological functions of astrocytes is presented to build a comprehensive view of the different functions, in addition to the modelling studies of astrocyte glutamate transport. Although this study is about glutamate transport, it is important to understand the other cellular processes as well since the cellular functions are in constant interaction and do not exist in isolation. After Literature Review, Objectives of the study are presented, followed by Materials and Methods, Results and Discussion, and ending with Conclusions.

2. LITERATURE REVIEW

2.1 Astrocyte Physiology

2.1.1 Glutamate Uptake

Glutamate transporters (Excitatory Amino Acid Transporters 1-5, EAAT1-5) are membrane proteins that couple the transport of glutamate (Glu^-) into the cell to the co-transport of 3 sodium (Na^+) ions and 1 hydrogen (H^+) ion and the counter-transport of 1 potassium (K^+) ion. Since glutamate is negatively charged, the net charge transferred to the cell in one transport cycle is +2. The transporter protein also forms an anion channel for the movement of chloride (Cl^-) ions, but the movement of these ions is independent of the glutamate transport (Untiet et al., 2017). The main type of transporter expressed in astrocytes is EAAT2, which is also called Glutamate Transporter 1 (GLT-1). Most glutamate transporters form a homotrimeric complex with a bowl-like structure (Figure 1), that allows the glutamate to diffuse into the structure and supports efficient transport (Vandenberg and Ryan, 2013).

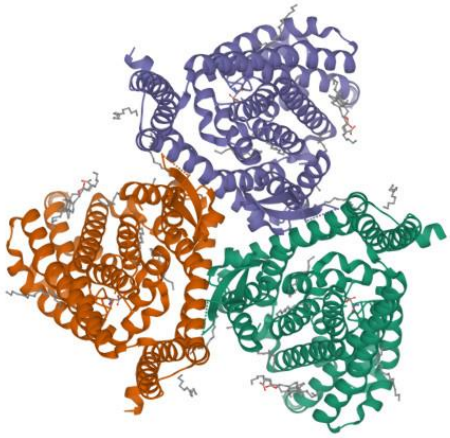

Figure 1. *Structure of human excitatory amino acid transporter 2. Image from the RCSB PDB (rcsb.org) of PDB ID 7XR4 (Originally published in Zhang et al., (2022). Structural basis of ligand binding modes of human EAAT2. Nat Commun, 13:3329-3329)*

The role of glial glutamate uptake has interested researchers for decades (Schousboe et al., 1977). Astrocytic glutamate transporters are important in the proper functioning of the brain. Knock-out of the transporters has been demonstrated to cause fatal epilepsy (Petr et al., 2015). The transporters clear glutamate from the synaptic cleft and they may also influence synaptic transmission, in addition to preventing excitotoxicity and providing glutamate for the glutamine conversion and energy production (Takahashi et al., 2015). Several mechanisms have been found to inhibit glutamate uptake, including cellular depolarization, increased extracellular K^+ levels ($[K^+]_o$) and adenosine receptor activation (Armbruster et al., 2022; Matos et al., 2013; Rimmele et al., 2017).

Previously, it has been thought that the astrocyte membrane potential is quite stable, but recent evidence indicates that local membrane potential changes can be in the order of 20 mV, and depolarizations inhibit glutamate uptake (Armbruster et al., 2022). The cause of the depolarizations is the increased $[K^+]_o$ and the glutamate transporter activity. The inhibiting effect of increased $[K^+]_o$ on transporter function was reported by Rimmele et al. (2017), who present a neuromodulatory mechanism involving decreased transporter activity and increased presynaptic metabotropic glutamate receptor (mGluR) activation. The functioning of glutamate transporters relies on the ion concentration gradients because it is a secondary active transporter, which uses the gradient produced by primary active transporters, to transport glutamate. An inhibitory mechanism has been found, where the activity of the Na^+/K^+-Adenosine triphosphatase (Na^+/K^+-ATPase) is decreased by activation of adenosine A_{2A} receptors, inhibiting glutamate uptake (Matos et al., 2013).

The inhibition of the glutamate transporter function is one modulatory mechanism affecting the transporter itself, but in addition we can consider how the normal functioning of the transporters affects intracellular events in astrocytes. This question is still largely unanswered, but there have been studies investigating the relationship between glutamate transporters and Ca^{2+} events (Ibáñez et al., 2019; Kirischuk et al., 2007; Oschmann et al., 2017; Rojas et al., 2007). The source of Ca^{2+} increase in the cytosol could be the cell membrane Na^+-Ca^{2+} exchanger (NCX). This transporter could respond to the rise in intracellular Na^+ concentration caused by the operation of glutamate transporters (Figure 2). The Ca^{2+} signal would then be generated by the reverse operation mode of NCX, when it removes Na^+ from the cell while transporting Ca^{2+} into the cell. There is also evidence that long periods of reverse activity of NCX would result in Ca^{2+} release from the endoplasmic reticulum (ER), in a process called Ca^{2+}-induced Ca^{2+} release (CICR)

(Rojas et al., 2007). The release of Ca^{2+} from the ER could further activate cell membrane channels called store-operated Ca^{2+} channels (SOCC).

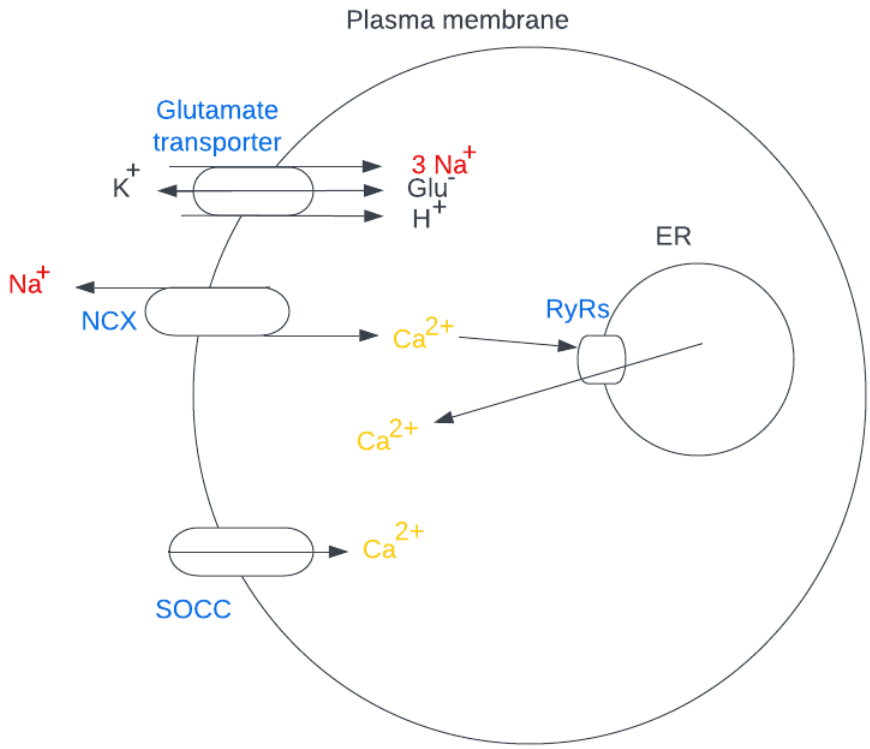

Figure 2. *The connection between glutamate transporter and NCX. Glutamate transporter function results in an increase of intracellular Na^+. This reverses NCX function, resulting in Ca^{2+} entry to the cell. Ca^{2+} activates ER receptors, which results in Ca^{2+} release from the ER and amplification of the Ca^{2+} signal. SOCC channels in the plasma membrane are also activated after the release of Ca^{2+} from the ER. Modified from Rojas et al. (2007).*

Another intracellular effect of glutamate transporter function is that the movement of mitochondria decreases, and mitochondria place themselves close to the transporters (Jackson et al., 2014). In the study of Jackson et al. (2014), they also found that when the reverse operation of NCX was blocked, mitochondria were more mobile than during the normal neural activity and glutamate transporter function. This links again the function of glutamate transporter and NCX.

Besides the intracellular mechanisms, it is also of interest to know the effects of glutamate transport on brain networks and brain function in general. The most obvious effect is on the synapse level, where the transporters directly affect the glutamate concentration in the synaptic cleft. This concentration defines how different receptors, located both on

neuronal and astrocytic membranes, get activated. Thus, the glutamate transporters fundamentally affect synaptic transmission. As an example of the importance of the transporters to the network function and development, it has been observed that in the visual cortex, in conditions of lowered expression of the transporter, the relationship between ipsilateral and contralateral inputs of the eye develops abnormally (Sipe et al., 2021). Restoring astrocyte glutamate uptake is also important when considering the repair of injured central nervous system. For example, in the development of biomaterials, the effects of these materials on astrocytes could be assessed by looking at the expression of glutamate transporters. Zuidema et al. (2014) found that electrospun poly-l-lactic acid fibers have beneficial effects on glial cells and enhance glutamate uptake.

2.1.2 Potassium Buffering

Potassium is released to the extracellular space during neuronal activity and one of the functions of astrocytes is to clear and buffer K^+. The K^+ buffering hypothesis was formed during 1960–1970 (Abbott and Pichon, 1976). The key proteins in this process are inwardly rectifying K^+ ($K_{ir}4.1$) cell membrane channels. In resting conditions, the cell membrane potential is more positive than the equilibrium potential for K^+, meaning that K^+ ions tend to move out of the cells. When $[K^+]_o$ increases, the equilibrium potential for K^+ increases, which results in depolarization, and the membrane potential increases (Bellot-Saez et al., 2017). K^+ influx will happen if the equilibrium potential for K^+ is greater than the membrane potential. The special property of astrocytes is that through gap junctions they can have isopotentiality. This means that local depolarization is small and the membrane potential does not change much, enabling the K^+ influx to continue as long as the $[K^+]_o$ remains elevated. The increases of $[K^+]_o$ can be highly local, and the same is true for the resulting astrocyte depolarizations, which can be very local (Armbruster et al., 2022).

In addition to K_{ir}- and gap junction -mediated K^+ spatial buffering, K^+ can be actively transported to the cell via Na^+/K^+-ATPase (Bellot-Saez et al., 2017). Both spatial buffering and active transport of K^+ affect neuronal excitability. To study network activity and investigate the relationship between neuronal spiking and glial cell responses, Wanke et al. (2016) used microelectrode array (MEA) recordings and developed a procedure to separate different events from the MEA signal. The K^+ currents that were detected, had different directions (out->in or in->out) depending on whether there were neuronal spikes present. This is in line with the K^+ buffering model.

Disruptions in the K^+ clearing capabilities are observed in various diseases. Abnormalities in the function of $K_{ir}4.1$ have been found in epilepsy. Downregulation of the protein has been observed in epilepsy patients and additionally, mutations in the gene *KCNJ10* which encodes $K_{ir}4.1$, are associated with seizure phenotypes (Steinhäuser et al., 2012). If $[K^+]_o$ levels stay elevated, it will cause the membrane potential of neurons to increase, thus allowing easier activation of ion channels. The effect can also be seen in astrocytes, where blockage of $K_{ir}4.1$ increases perisynaptic astrocyte process depolarization (Armbruster et al., 2022).

2.1.3 Ion and Water Homeostasis

The K^+ buffering discussed in Section 2.1.2 is one type of mechanism for ion homeostasis, and possibly one of the most critical ones, but there are also other homeostasis mechanisms which control for example extracellular pH and volume. The ion homeostasis is closely linked to the water homeostasis (Olson and Evers, 1992). Ions accumulate in astrocytes following neuronal activity, for example through K^+ buffering or Na^+ influx which is coupled to many transporter functions. This causes astrocyte swelling according to osmosis rules. To counteract the swelling, a process called regulatory volume decrease (RVD) is activated. The ion channels important in RVD are volume-regulated anion channels (VRAC), which allow the efflux of anions (Min and van der Knaap, 2018). Water movement across the membrane in astrocytes is enabled by aquaporin 4 (AQP4). Different isoforms of AQP4 exist, and the isoforms AQP4a, AQP4c and AQP4e assemble into plasma membrane structures called orthogonal arrays of particles (OAPs) (Lisjak et al., 2017).

Although astrocytes do not generate Na^+/K^+-based action potentials, the steep gradients of Na^+ and K^+ ions across the membrane also exist in these cells. The key generator of the gradient is the same, the Na^+/K^+-ATPase. When Na^+ gradient is used by transporters, Na^+/K^+-ATPase restores the gradient. It is also possible for many transporters to reverse, and thus transport Na^+ out of the cell. Na^+ homeostasis should then be thought of as a process where Na^+ fluctuations occur, and different influx and efflux pathways play a role (Rose and Karus, 2013).

Na^+ and K^+ are among the most significant ions, whose concentration is regulated in the brain, but many different inorganic (e.g., Ca^{2+}) and organic ions exist. For example, glutamate is the anion form of glutamic acid, as discussed in Section 2.1.1. It has been

identified that metal ion homeostasis (zinc, copper) in astrocytes is upregulated in Alzheimer's disease (AD), providing protection for the cells (Smith et al., 2022). However, the big picture is that astrocytes form networks, also connecting with oligodendrocytes to form panglial syncytium, and making connections with their endfeet structures for example to vasculature. The panglial syncytium is important in maintaining homeostasis over broad areas of the brain and the endfeet connections allow to exchange ions and water with non-neuronal elements (Min and van der Knaap, 2018).

2.1.4 Calcium Signalling

Astrocyte Ca^{2+} signalling has been thought of as the main signalling mechanism of astrocytes. The central protein in Ca^{2+} signalling, Ca^{2+}-calmodulin dependent protein kinase, was found in astrocytes, though later than in neurons (Babcock-Atkinson et al., 1989). The possible sources of Ca^{2+} signal are the inositol-trisphosphate (IP_3) dependent release from the ER, release from mitochondria, or Ca^{2+} entry through cell membrane channels (Figure 3) (Okubo, 2020). The release of Ca^{2+} from the ER can happen via two different receptors which allow the Ca^{2+} flux. One of them is the ryanodine receptor (RyR), which works as a Ca^{2+} channel after Ca^{2+} has bound to it, being involved in the process of CICR. The other ER receptor is the IP_3 receptor (IP_3R), which also needs to bind Ca^{2+} to get activated, but in addition it needs to bind IP_3. The IP_3 signal is created when a G-protein coupled receptor (GPCR) on the cell membrane binds some extracellular ligand, for example glutamate. The other possible sources of Ca^{2+} signals are release from mitochondria through the mitochondrial permeability transition pore (mPTP) and Ca^{2+} entry through cell membrane Ca^{2+} channels.

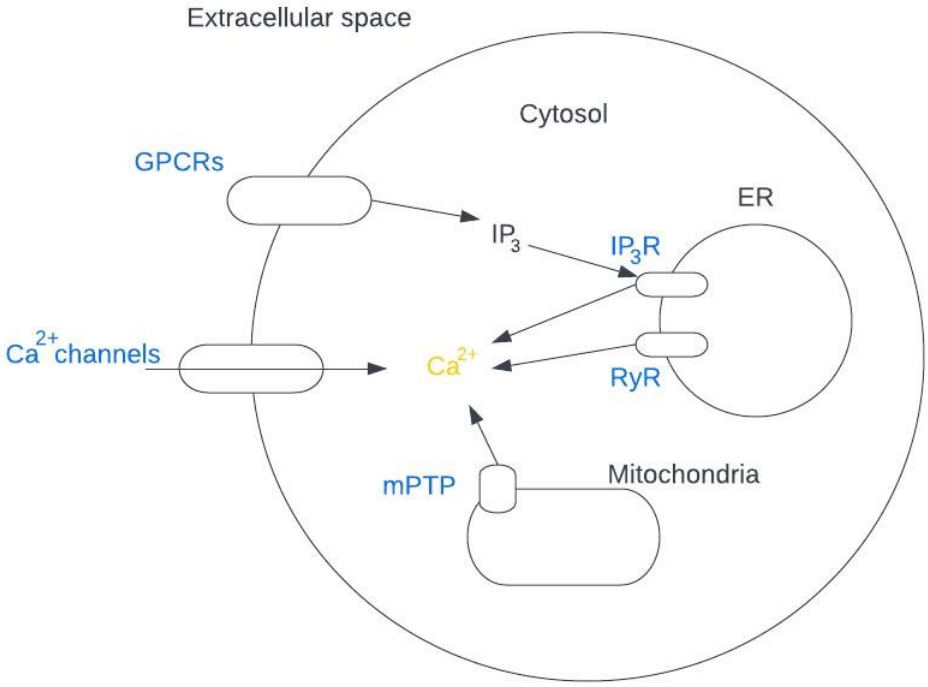

Figure 3. *Different sources of Ca^{2+} signal. Ca^{2+} can be released from the ER via two different receptors: IP_3R and RyR. IP_3R requires activation of the receptor by IP_3, which is formed after GPCR gets activated on the cell membrane. Other Ca^{2+} entry pathways include cell membrane Ca^{2+} channels and release from mitochondria via mPTP. Modified from Okubo (2020).*

One also somewhat controversial event resulting from Ca^{2+} signalling in astrocytes is the release of gliotransmitters, for example glutamate. The release of glutamate from astrocytes in response to Ca^{2+} signals has been suggested to contribute to epileptic seizures and the synchronous neuronal activity observed in epilepsy (Carmignoto and Haydon, 2012). It has been observed that when the network is hyperexcited, astrocytes respond to that with significant Ca^{2+} increases, which would then result in the release of glutamate, and promote even stronger excitation. But what is the role of Ca^{2+} signalling in normal conditions? It has been linked to the communication between neurons and astrocytes, but a lot is still to be learned. Yu et al. (2018) studied the effect of reducing Ca^{2+} signalling in an *in vivo* study conducted in striatum. The study showed that the reduced signalling affected neuronal activity and resulted in repetitive self-grooming behaviours in mice. The proposed mechanism behind this was that when Ca^{2+} signalling was reduced, GABA transporter (GAT) was too active, which caused the lowering of GABA concentration in the extracellular space.

Regarding the regulators of Ca^{2+} signalling in astrocytes, it was recently found that the protein kinase-D interacting substrate of 220 kDa (Kidins220) is needed for both spontaneous and stimulus-induced Ca^{2+} signals in embryonic astrocytes (Jaudon et al., 2020). The study also showed that with the knock-out of Kidins220 in embryonic astrocytes, neuronal development was disturbed. Although experimental data of Ca^{2+} signals is available, to really understand the meaning of these signals, progress in Ca^{2+} imaging methods and *in silico* work is needed (Rusakov, 2015; Semyanov et al., 2020).

2.1.5 Energy Metabolism

Energy metabolism includes the vital processes of aerobic and anaerobic respiration that generate ATP, and fatty acid and amino acid metabolism. The main source of energy in astrocytes is glucose which astrocytes use in two ways. The usual tricarboxylic acid (TCA) cycle and oxidative phosphorylation take place in mitochondria, but in addition the glycolysis pathway in cytoplasm is used to produce lactate even in aerobic conditions (Chatton et al., 2016). Astrocyte metabolism is linked to the metabolism of neurons. The concept of astrocyte-neuron metabolic unit is not new, since it has already been used in earlier studies of energy metabolism in pathologic conditions (Miquel and Haymaker, 1965). There is evidence of an existing astrocyte-neuron lactate shuttle (ANLS), in which astrocytes release lactate to neurons in response to activity (Beard et al., 2022). However, the existence of ANLS is still controversial. Astrocyte energy metabolism is activated by increases in intracellular Na^+ concentration, which happens when different transporters use the Na^+ gradient to transport ions or molecules, such as glutamate, inside the cell (Chatton et al., 2016). The energy metabolism is closely linked to the neurotransmitter metabolism, since the glutamate that is transported to the cell can either be converted to glutamine and contribute to the glutamate-glutamine cycle, or it can be fed into the TCA cycle by converting it to α-Keto-glutarate.

It is of interest to consider the whole brain energy metabolism, which includes the energy consumption and production by different cell types, namely neurons, glial cells, and endothelial cells. The exact mechanisms of metabolic interaction between these cell types are still not fully understood, but some concepts have been uncovered. Astrocytes have been thought to be integral in the coordination of brain energy demands. The reason for this is that astrocytes are in contact with both the synapses and the vasculature (Byrne and Roberts, 2004). Thus, they are well equipped to sense changes in energy demands

and adapt to that (Jolivet et al., 2015; Nortley and Attwell, 2017). As proposed by Chatton, Magistretti and Barros (2016), Na^+ could be the “energy currency”, which is important in metabolic signalling. Because astrocytes are connected through gap junctions, Na^+ and for example lactate can be spatially distributed.

Astrocyte energy metabolism has relevance in AD and epilepsy. In AD, astrocyte metabolism is altered, which can have effects on the glutamate-glutamine cycle. One mechanism could be that when the energy production through glycolysis and oxidative phosphorylation is disrupted, the Na^+/K^+-ATPase does not function properly, meaning that the glutamate transporter function is also limited (Andersen et al., 2022). In a large proteomic study of AD, an increase in astrocyte and microglial energy metabolism associated proteins was found and the proteins were among the ones that were most significantly associated with AD (Johnson et al., 2020). However, Johnson et al. propose a neuroprotective role for these proteins, so there are still uncertainties about the impact of the changes in astrocyte metabolism. In epilepsy, the glutamate concentration in the synapses increases, and when astrocytes transport glutamate into the cell, it triggers glycolysis and production of lactate, which is then supplied to neurons. Astrocytes thus support the energy demands of neurons in the epileptic state (Boison and Steinhäuser, 2018). Also, the dysfunction of astrocyte gap junctions has been observed in epilepsy, which on the one hand restricts energy metabolite movement and could be anti-epileptic, but on the other hand negatively affects the K^+ buffering capabilities, which would promote epileptic states (Mazaud et al., 2021).

2.1.6 Astrocyte-Neuron Interactions

Astrocytes and neurons are physically close to each other and share the same extracellular space. The structural interactions between astrocytes and neurons were observed earlier, and later the potential functional interactions caught the attention of researchers (Hertz, 1979). The physiological events that occur in astrocytes can have an impact on neurons. For example, in the above sections where astrocyte glutamate uptake, K^+ buffering, ion and water homeostasis, Ca^{2+} signalling and energy metabolism are reviewed, the effects on neurons are also discussed. In a synapse level the structure is called a tripartite synapse, in which there is a presynaptic nerve terminal, a postsynaptic dendrite and an astrocyte process. This concept of a tripartite synapse is bringing more focus to

the role of astrocytes in the synaptic function than the traditional description of a synapse that exists between two neurons (Araque et al., 1999). Although the role of astrocytes is recognized and new results of their contribution to synaptic function is accumulating, there remains a lot to be understood about the exact molecular mechanisms.

One type of possible interaction between neurons and astrocytes is the activation of astrocytic cell membrane receptors, which then results in activation of Ca^{2+} signalling pathways in astrocytes. This signalling can be measured as a Ca^{2+} signal and it can induce the release of gliotransmitters, which then influence neurons. This type of mechanism has been observed in spike-timing-dependent plasticity (STDP). In the study of Min and Nevian (2012), astrocytes were found to be essential for the formation of long-term depression (LTD) in the rat barrel cortex layer 4 – layer 2/3 synapse. In this type of LTD, astrocytes received the signal through endocannabinoid receptors, which resulted in a Ca^{2+} signalling cascade that eventually resulted in the release of glutamate.

Other examples of astrocyte-neuron interactions have been observed, which are not part of STDP. In substantia gelatinosa of the spinal cord dorsal horn, astrocytes received a signal through P2X purinoceptor 7 (P2X7 receptors) and released glutamate (Ficker et al., 2014). This interaction is thought to occur in pathological conditions, and specifically in pain processing. In striatum, an interaction between astrocytes and neurons was studied in the context of alcohol use disorder (Hong et al., 2021). It has been observed that astrocyte Ca^{2+} signalling affected the neurons in the striatum and even the behaviour of animals (Yu et al., 2018). These striatal astrocytes might play a role in reward-seeking behaviour through adenosine signalling (Hong et al., 2021).

In a stem cell model of Down syndrome, a neuron-astrocyte interaction has been found, where spontaneous Ca^{2+} signals of astrocytes reduced the excitability of neurons (Mizuno et al., 2018). This type of interaction is different compared to the above discussion, since here the Ca^{2+} signals that affect the neurons are spontaneous, and not caused by activation of some receptors. The possible cause of the spontaneous Ca^{2+} signalling in astrocytes was found to be overexpression of a protein S100B (Mizuno et al., 2018). Another new astrocyte-neuron interaction was studied in normal astrocytes in brain slices. In this interaction, astrocyte processes depolarized after neuronal activity, which inhibited glutamate clearance, and thus allowed neurons to get activated (Armbruster et al., 2022). Astrocyte membrane potential has been thought to be stable, but the results of Armbruster et al. (2022) revealed that the depolarizations of astrocyte processes can be significant, and they can have consequences that influence neurons.

2.1.7 Control of Blood Flow

Blood flow regulation in the brain is necessary, so that oxygen and nutrients can be supplied to the brain region where there is activity and energy is needed. The so-called neurovascular unit controls the blood flow, and it includes astrocytes, vascular smooth muscle cells, pericytes and endothelial cells (Kisler et al., 2017). In 1987, Paulson and Newman wrote an article with a title: “Does the Release of Potassium from Astrocyte Endfeet Regulate Blood Flow?”. As of today, the mechanisms of blood flow regulation are still not clear. Two regulatory mechanisms can be separated. One is the vasodilation that is activity-dependent, and the other is the tonic regulation in resting conditions. The tonic regulation by astrocytes is dependent on their resting intracellular Ca^{2+} levels and the release of prostaglandins (Rosenegger et al., 2015). Increase in Ca^{2+} and the release of prostaglandins were also identified as the mechanisms of astrocytes that cause vasodilation in hypoglycemia (Nippert et al., 2022). It has also been shown that astrocytes have homeostatic roles in the control of blood flow and they respond to low blood pressure by activating circuits that increase the pressure and heart rate (Marina et al., 2020).

However, there are still controversies regarding the role of astrocytes in the control of blood flow. It seems that one key controversy is about the role of Ca^{2+} signalling in astrocytes. There are even opposite results, where some studies found the increase in Ca^{2+} to be involved in vasoconstriction and others in vasodilation (Kisler et al., 2017). Some recent studies support the astrocyte contribution to vasodilation. In one study, vasodilation significantly decreased in IP_3R type 2 (IP_3R2) knockout mice, which provides evidence for the Ca^{2+}-dependence of vasodilation (Nippert et al., 2022). In another study, Ca^{2+} contributed to vasodilation, and decreasing the resting Ca^{2+} levels in astrocytes caused vasoconstriction (Rosenegger et al., 2015). One hypothesis is also that the effect of Ca^{2+} signal depends on the region where the astrocyte is (Figure 4). Astrocyte Ca^{2+} signalling has also been observed in response to decreased cerebral perfusion pressure, and if Ca^{2+} signalling was blocked, it prevented the compensatory increase in the pressure (Marina et al., 2020).

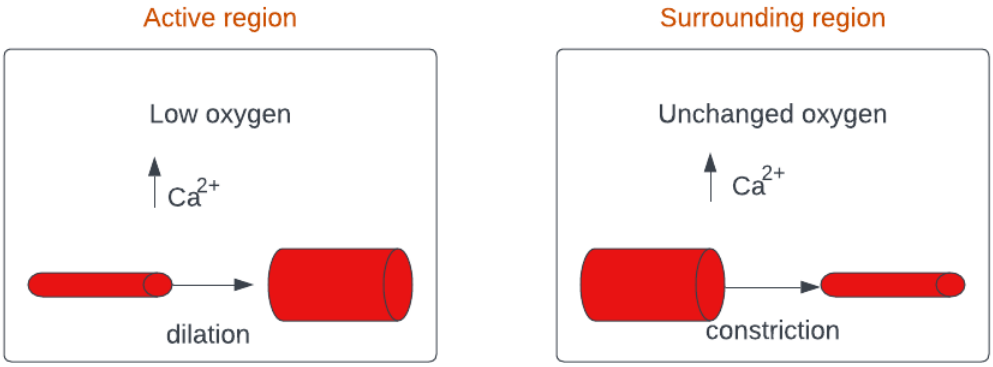

Figure 4. *Astrocyte Ca^{2+} signalling can have different effects on the vasculature depending on the region. Several hypotheses have been presented. According to one of the hypotheses, increase in astrocytic Ca^{2+} causes vasodilation in the active region, where oxygen is low (Carmignoto and Gómez-Gonzalo, 2010; Lu et al., 2019). In contrast, an increase in astrocytic Ca^{2+} can cause vasoconstriction in the surrounding region, where oxygen levels are unaffected (Carmignoto and Gómez-Gonzalo, 2010; Kim et al., 2015). Modified from Carmignoto and Gómez-Gonzalo (2010).*

One disease where cerebral blood flow is disturbed is AD. There is a so-called two-hit hypothesis that acts on the vasculature in AD. These two hits are amyloid beta (Aβ)-independent and Aβ-dependent mechanisms, which involve many factors and different cell types (Kisler et al., 2017). Regarding astrocytes, the activation of these cells and the resulting inflammation is part of the pathogenesis.

2.1.8 Astrocytes and the Endocrine System

Endocrine glands secrete hormones to control the homeostasis of our bodies. The neuroendocrine system involves the hypothalamus and the pituitary gland. Hypothalamus releases neuropeptides, which target the pituitary gland, and result in the release of hormones from the pituitary gland. These hormones then have different target tissues in the periphery. In the past, astrocytes were not thought to be important for the neuroendocrine system, but now there is evidence of their contribution (Chowen et al., 2016). Also, for example Schipper wrote already in 1991 that Gomori-positive astrocytes could be involved in neuroendocrine disorders (Schipper, 1991). When astrocytes are considered in the context of the endocrine system, it is possible to examine how they influence the

neuroendocrine system function and how they are influenced by hormones that are released in the periphery. There are studies of the interactions between astrocytes and the metabolic and reproductive hormones (gonadal steroid hormones).

The main gonadal steroid hormones are estradiol, progesterone, and testosterone. These hormones can cross the blood brain barrier and have effects on astrocytes through receptors. Astrocytes are even able to produce steroid hormones. For example, estradiol can activate through the estrogen receptor the production of progesterone in astrocytes of the hypothalamus (Acaz-Fonseca et al., 2016). An interesting finding is that insulin, which is a metabolic hormone, is needed to be sensed by astrocytes for the correct function of the reproductive system, since knocking-out the insulin receptor in astrocytes resulted in defects of the reproductive axis and fertility (Manaserh et al., 2019). Gonadal steroid hormones affect astrocytes in physiological and pathological conditions. In physiological conditions they regulate glial fibrillary acidic protein (GFAP) expression and astrocyte morphology (Acaz-Fonseca et al., 2016). GFAP regulation is also relevant in pathological conditions. In those conditions, gonadal steroid hormones have effects on astrocyte reactivity by downregulating gliosis and promoting tissue repair (Acaz-Fonseca et al., 2016).

Hypothalamus is the key structure in the brain for the control of metabolic homeostasis in the whole body. It receives nutritional signals (e.g., glucose and fatty acids) and hormones (e.g., leptin and ghrelin) which then affect the hypothalamic response to maintain homeostasis. Evidence is being accumulated on astrocytes' role in this response. For example, astrocytes respond to leptin by changing synaptic activity in the hypothalamus (Chowen et al., 2016). It was also found that lipoprotein lipase (LPL) in hypothalamic astrocytes contributes to metabolic regulation (Gao et al., 2017). Mice that lacked LPL gained more body weight and developed glucose intolerance in high-fat diet conditions. Other mechanisms that astrocytes have that could affect metabolic control are the release of signalling molecules such as cytokines, changes in astrocyte coverage of the neurons and stimulation of the feeling of fullness through apolipoprotein E (Chowen et al., 2016). Although the role of astrocytes in the hypothalamic control of metabolism is not well characterized, the fact that astrocytes transport nutrients from the vasculature, and are able to affect synaptic transmission, makes it possible for them to play a role in the hypothalamic response.

2.1.9 Epilepsy

Epilepsy is one neurological disease, where astrocyte contribution is acknowledged. In the past, it was thought that reactive astrocytes are not able to clear K^+ which results in hyperexcitability of neurons (Pollen, 1973). In fact, many of the physiological processes of astrocytes may be involved, including glutamate transport, K^+ buffering, Ca^{2+} signalling and energy metabolism. Vascular mechanisms are also involved, and disruptions in blood–brain barrier can be seen as the root cause of changes that are observed in epilepsy (Figure 5). The proposed mechanism involves a serum protein, albumin, which can activate transforming growth factor β (TGFβ) signalling in astrocytes, resulting in dysfunction of various astrocyte proteins (Heinemann et al., 2012).

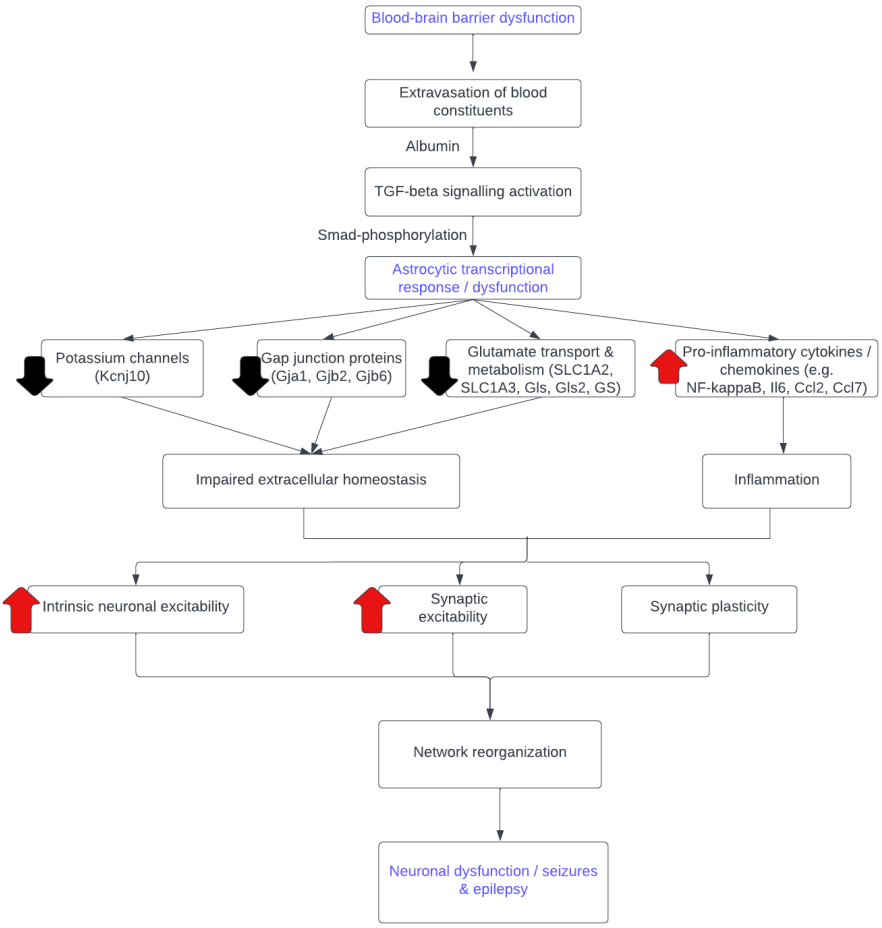

Figure 5. *Diagram of the events that could explain astrocyte contribution to epileptogenesis. The root cause presented here is blood–brain barrier dysfunction which leads to astrocytic transcriptional responses. These responses influence neurons and the networks they form, resulting in neuronal dysfunction and seizures (Purnell et al., 2023). Modified from Heinemann et al., (2012).*

As can be seen in Figure 5, there is also a potential contribution of astrocyte inflammatory responses. While microglia are thought to be the main immune cells of the central nervous system, astrocyte immune responses are observed in different diseases, including epilepsy. When astrocytes get activated, they can express inflammatory molecules and also their receptors, for example interleukin-1β (IL-1β) and its receptor ILR1 (Aronica et al., 2012). This means that astrocytes are both producers and targets of inflammatory molecules. The cytokines and chemokines produced in astrocytes may have effects on neuronal excitability (Heinemann et al., 2012). IL-1β can affect both neuronal and astrocytic mechanisms. In astrocytes, it can inhibit glutamate uptake and promote glutamate release, while in neurons, it has been observed to increase N-methyl-D-aspartate (NMDA) receptor function (Aronica et al., 2012).

The role of astrocyte gap junctions in epilepsy is not clear. The disturbance of gap junctions would affect the K^+ clearance capabilities negatively and thus promote the excitability of neurons (Steinhäuser et al., 2012). But in addition, the movement of energy substrates would also be prevented, which would impair the energy supply for neurons. Nevertheless, the gap junction uncoupling could be a potential mechanism that is relevant for epilepsy. Interestingly, it has been found that astrocyte alkalization precedes the gap junction uncoupling, and it can be prevented by blocking the Na^+/bicarbonate (Na^+/HCO_3^-) cotransporter (Onodera et al., 2021).

Glutamate transporter dysfunction is also a potential mechanism observed in epilepsy. The transporter genes (*slc1a2* and *slc1a3*) are downregulated in astrocytes in epilepsy (Heinemann et al., 2012). It is intuitive that abnormal glutamate transporter function contributes to the disease, since epilepsy is characterised by hyperexcitability, and the transporters have a direct effect on the synaptic glutamate concentration. Deletion of the transporter in astrocytes results in seizures and increased mortality (Petr et al., 2015). The opposite effect is achieved by overexpressing the transporter, which decreases the number of seizures (Peterson et al., 2021). This means that astrocyte glutamate transporters are a potential therapeutic target in epilepsy. Astrocytes might also have an intrinsic mechanism to increase their glutamate transporter function in epileptic conditions. There is evidence from adult mice (between 8 and 14 weeks) that metabotropic glutamate receptor mGluR5 expression emerges in epilepsy, and the potential function of it is to enhance glutamate uptake in high-frequency stimulus conditions (Umpierre et al., 2019).

2.1.10 Summary

In the above sections, different aspects of astrocyte physiology and underlying mechanisms are presented. There are numerous molecular mechanisms that enable these physiological processes, but especially relevant are the membrane mechanisms. These mechanisms include cell membrane proteins, which are channels, transporters, or receptors. They allow the cells to interact with their surroundings and control the extracellular and intracellular environment. Different channels, transporters and receptors that have been found in astrocyte membranes are collected in tabular format (Table 1, Table 2 and Table 3). These membrane proteins have been found in astrocytes at various locations of the central nervous system and in diverse conditions (for example in different developmental stages, species, and diseased or healthy tissue). Thus, not all of them are expressed in every astrocyte.

Astrocytes are involved in many physiological processes in the brain, ranging from ion control and homeostasis mechanisms to signaling mechanisms affecting the neighboring neurons, energy metabolism, endocrine system, and vascular system function. The contribution of astrocytes to many diseases is also recognized. In addition to epilepsy, many neuropsychiatric and neurological diseases have an astrocyte contribution to the disease development. There is also variation in how established a certain function of astrocytes is. The K^+ buffering hypothesis goes back to 1960's (Bellot-Saez et al., 2017), but many other functions are not as established and the research is still ongoing. The evidence is also acquired with different research methods, which affects the reliability of the results. Some results are only from *in vitro* studies but having studies from slices and *in vivo* adds more confidence to the findings. For a single physiological process, many membrane mechanisms and intracellular mechanisms work together to achieve the correct function. Additionally, the different physiological processes affect each other. Many of the details of this interplay are still not fully understood, and computational modeling is one approach to study this.

Table 1. *Ion channels in astrocytes. Physiological process is only given when there is a direct relation to a process discussed in above sections. The horizontal lines in the table are only for making the table easier to read.*

Ion Channel	Function	Physiological Process	Reference
ATP-sensitive K^+ channel (K-ATP)	K^+ channel		(Wang et al., 2022)
Aquaporin (AQP)	Water channel	Water homeostasis, epilepsy	(Kettenmann, 2013)
ATP-dependent, nonselective cation channel (NCCa-ATP)	Cation channel		(Jayakumar et al., 2014)
Ca^{2+}-activated Cl^- channel (CAAC)	Anion channel	Neuron-astrocyte interaction	(Kettenmann, 2013)
Epithelial Na^+ channel	Na^+ channel		(Verkhratsky and Nedergaard, 2018)
Hemichannel	Two hemichannels can form a gap junction, but hemichannel can also be a channel between cytosol and extracellular space	Ion homeostasis, Ca^{2+} signalling, K^+ buffering, epilepsy, energy metabolism	(Olsen et al., 2015)
Inwardly rectifying K^+ channel (K_{ir})	K^+ channel	K^+ buffering, epilepsy	(Kettenmann, 2013)
Large-conductance Ca^{2+}-activated K^+ channel (BK/K_{Ca}1.1)	K^+ channel	Control of blood flow	(Kettenmann, 2013)
Maxi-anion channel	Anion channel		(Zhao et al., 2017)
Na_x channel	Na^+ channel		(Verkhratsky and Nedergaard, 2018)

Table 1 (continued).

Olfactory-type cyclic nucleotide gated channel (CNG)	Cation channel		(Podda et al., 2012)
Ca^{2+} release-activated Ca^{2+} channels	Ca^{2+} channels	Ca^{2+} signalling	(Verkhratsky and Nedergaard, 2018)
Pannexin 1 channel	Membrane channel		(Silverman et al., 2009)
Piezo1&2 mechanosensitive ion channel	Mechanosensitive cation channel		(Choi et al., 2015)
Small conductance Ca^{2+} activated K^+ channel (SK/K_{Ca})	K^+ channel	Control of blood flow	(Kettenmann, 2013)
Transient receptor potential channel (TRP)	Cation channel	Ca^{2+} signalling, ion homeostasis	(Kettenmann, 2013)
Two-pore domain K^+ channel	K^+ channel/ cation channel	K^+ buffering	(Olsen et al., 2015)
Voltage-activated K^+ channel (K_v)	K^+ channel		(Kettenmann, 2013)
Voltage-gated anion channel (ClC)	Cl^- channel or Cl^- / H^+ exchanger		(Kettenmann, 2013)
Voltage-gated Ca^{2+} channel (Ca_v)	Ca^{2+} channel	Ca^{2+} signalling	(Kettenmann, 2013)
Voltage-gated Na^+ channel (Na_v)	Na^+ channel		(Kettenmann, 2013)
Volume-regulated anion channel (VRAC)/volume-sensitive outwardly rectifying channel (VSOR)	Anion channel	Water homeostasis	(Kettenmann, 2013)

Table 2. *Transporters in astrocytes. Physiological process is only given when there is a direct relation to a process discussed in above sections. The horizontal lines in the table are only for making the table easier to read.*

Transporter	Function	Physiological Process	Reference
ATP-binding cassette transporter A1 (ABCA1)	Transport of cholesterol and neutral lipids		(Sato et al., 2007)
Carnitine transporter (OCTN2)	Organic cation and carnitine transport	Energy metabolism	(Juraszek and Nałęcz, 2016)
Cationic amino acid transporter (Acs-1)	Transport of small neutral D- and L-amino acids		(Verkhratsky and Nedergaard, 2018)
Choline transporter-like protein 1 (CTL1)	Transport of choline and organic cations		(Inazu et al., 2005)
Concentrative nucleoside transporter	1 Na^+ and 1 nucleoside into the cell		(Verkhratsky and Nedergaard, 2018)
Equilibrative nucleoside transporter	Transport of adenosine		(Verkhratsky and Nedergaard, 2018)
GABA transporter (GAT)	1 GABA, 2 Na^+ and 1 Cl^- into the cell	Energy metabolism, epilepsy, neuron-astrocyte interactions	(Parpura and Haydon, 2009)
GLAST/EAAT1	1 glutamate, 3 Na^+ and 1 H^+ in, 1 K^+ out	Glutamate transport, epilepsy	(Parpura and Haydon, 2009)
GLT1/EAAT2	1 glutamate, 3 Na^+ and 1 H^+ in, 1 K^+ out	Glutamate transport, epilepsy	(Parpura and Haydon, 2009)
GLT1b/EAAT2b	1 glutamate, 3 Na^+ and 1 H^+ in, 1 K^+ out	Glutamate transport, epilepsy	(Parpura and Haydon, 2009)

Table 2 (continued).

Glucose transporter	Transport of glucose	Energy metabolism	(Verkhratsky and Nedergaard, 2018)
Glutamine transporter	Transport of glutamine out of the cell		(Benarroch, 2016)
Glycine transporter (GlyT)	1 glycine, 2 Na^+ and 1 Cl^- into the cell		(Parpura and Haydon, 2009)
H^+-peptide transporter (PEPT2)	Uptake of peptides		(Kettenmann, 2013)
K^+/Cl^- cotransporter (KCC)	1 K^+ and 1 Cl^- out of the cell		(Kettenmann, 2013)
Monocarboxylate transporter (MCT)	Transport of 1 monocarboxylate anion and 1 H^+	Energy metabolism	(Kettenmann, 2013)
Na^+/Ca^{2+} exchanger (NCX)	Transport of 1 Ca^{2+} and 3 Na^+ in opposite directions	Ion homeostasis, Ca^{2+} signalling	(Kettenmann, 2013)
Na^+/H^+ exchanger (NHE)	1 H^+ out, 1 Na^+ in	Ion homeostasis	(Kettenmann, 2013)
Na^+/HCO_3^- cotransporter (NBC)	Transport of 1 Na^+ and 2 HCO_3^-	Ion homeostasis	(Kettenmann, 2013)
Na^+-dependent ascorbic acid transporter (SVCT2)	2 Na^+ and 1 ascorbic acid into the cell		(Verkhratsky and Nedergaard, 2018)
Na^+-dependent dopamine transporter (DAT1)	1/2 Na^+, 1 dopamine and 1 Cl^- into the cell		(Verkhratsky and Nedergaard, 2018)
Na^+/K^+-ATPase	3 Na^+ out, 2 K^+ in	Ion homeostasis, energy metabolism	(Kettenmann, 2013)

Table 2 (continued).

Neutral amino acid transporter (SNAT)	1 amino acid and 1 Na^+ out, 1 H^+ in		(Kettenmann, 2013)
Neutral amino acid transporter subtype (ASCT2)	1 Na^+ and 1 D-serine into the cell		(Verkhratsky and Nedergaard, 2018)
Neutral and basic amino acid transporter (B0,+)	Transport of 1 Cl^-, 1 amino acid and 2 Na^+		(Samluk et al., 2010)
$Na^+/K^+/Cl^-$ cotransporter (NKCC)	1 Na^+, 1 K^+ and 2 Cl^- into the cell	Ion homeostasis, K^+ buffering	(Kettenmann, 2013)
Norepinephrine transporter (NET)	1 norepinephrine, 2 Na^+ and 1 Cl^- into the cell		(Verkhratsky and Nedergaard, 2018)
Plasma membrane ATP-driven Ca^{2+} pump (PMCA)	Transport of Ca^{2+} out of the cell		(Kettenmann, 2013)
Serotonin transporter (SERT)	Uptake of serotonin		(Malynn et al., 2013)
Na^+-dependent glucose transporter	1 glucose and 2 Na^+ into the cell		(Verkhratsky and Nedergaard, 2018)
Sxc^- cystine/glutamate antiporter	Transport of glutamate out of the cell, cystine into the cell	Epilepsy	(Verkhratsky and Nedergaard, 2018)
Zinc transporter (ZnT)	Transport of zinc		(Verkhratsky and Nedergaard, 2018)

Table 3. *Astrocytic receptors. Physiological process is only given when there is a direct relation to a process discussed in above sections. The horizontal lines in the table are only for making the table easier to read.*

Receptor	Function	Physiological Process	Reference
Adenosine (A_1, A_2, A_3) receptor	Affects either: 1) phospholipase C, IP_3 and Ca^{2+} release from the ER 2) synthesis of cAMP	Ca^{2+} signalling	(Parpura and Haydon, 2009)
Adrenergic receptor (IJ_1AR, IJ_2AR, b_1AR, b_2AR)	Affects phospholipase C, IP_3 and Ca^{2+} release from the ER	Ca^{2+} signalling	(Parpura and Haydon, 2009)
AMPA receptor	Glutamate receptor, $Na^+/K^+/Ca^{2+}$ channel		(Parpura and Haydon, 2009)
Angiotensin receptor (AT_1, AT_2)	Affects phospholipase C, IP_3 and Ca^{2+} release from the ER	Ca^{2+} signalling	(Parpura and Haydon, 2009)
Bradykinin receptor (B_1, B_2)	Affects phospholipase C, IP_3 and Ca^{2+} release from the ER	Ca^{2+} signalling	(Parpura and Haydon, 2009)
Ca^{2+}-sensing receptor (CaSR)	GPCR	Ca^{2+} signalling	(Dal Prà et al., 2014)
Cannabinoid (CB_1) receptor	GPCR	Ca^{2+} signalling, astrocyte-neuron interactions	(Verkhratsky and Nedergaard, 2018)
Cannabinoid-like (CB-like) receptor	GPCR / unknown receptors, inhibition of adenylyl cyclase, regulation of nitric oxide production, closing of gap junctions		(Stella, 2010)

Table 3 (continued).

Chemokine receptor (CXCR2, CXCR4, CCR1, CCR2, CCR3, CCR5, CCR10, CCR11, CX3CR1)	GPCR	Ca^{2+} signalling	(Liu et al., 2014)
Class-A scavenger receptor (SR-A)	Involved in Aβ uptake by endocytosis		(Durand et al., 2019)
Complement 5a-like receptor (C5L2)	GPCR		(Gavrilyuk et al., 2005)
Cysteinyl leukotrienes receptor (CysLT1, CysLT2)	GPCR		(Huang et al., 2008)
Dopamine receptor (D_1, D_2, D_3, D_4)	Synthesis of cAMP	Ca^{2+} signalling	(Parpura and Haydon, 2009), (O'Connor et al., 2018), (Montoya et al., 2019)
Endothelin receptor	Increase in Ca^{2+}, opening of K^+ channel		(Kettenmann, 2013)
Prostaglandin E receptor 3 (EP3)	Prostaglandin receptor, causes a decrease in cAMP		(Paniagua-Herranz et al., 2017)
Ephrin receptor (Eph)	Receptor tyrosine kinase	Astrocyte-neuron interaction	(Murai and Pasquale, 2011)
Epidermal growth factor receptor (EGFR)	Causes phosphorylation of receptor tyrosine kinases, which leads to intracellular signalling		(Li et al., 2008)
Receptor tyrosine-protein kinase (erbB2, erbB4)	Receptor tyrosine kinase, neuregulin receptor	Astrocyte-neuron interaction	(Prevot et al., 2003)
Estrogen receptor α (ERα)	Nuclear receptor, but has also been found to localize to the cell membrane	Neuroendocrine system	(Sato et al., 2003)

Table 3 (continued).

Fibroblast growth factor receptor 1 (FGFR1)	Tyrosine protein kinase		(Iseki et al., 2002)
G protein-coupled estrogen receptor (GPER-/GPR-30)	GPCR	Neuroendocrine system	(Ibrahim et al., 2019)
GPCR GPR37-like 1 (GPR37L1)	GPCR		(Jolly et al., 2018)
$GABA_A$ receptor	Cl^- channel, Cl^- efflux		(Parpura and Haydon, 2009)
$GABA_B$ receptors	Affects phospholipase C, IP_3 and Ca^{2+} release from the ER	Ca^{2+} signalling	(Parpura and Haydon, 2009)
Glucagon-like peptide-1 receptor (GLP-1R)	Increase in cAMP	Energy metabolism	(Reiner et al., 2016)
Glutamate receptor (mGluRs)	Affects either: 1) phospholipase C, IP_3 and Ca^{2+} release from the ER 2) synthesis of cAMP	Ca^{2+} signalling, astrocyte-neuron interactions, epilepsy	(Parpura and Haydon, 2009)
Glycine receptor	Cl^- channel, Cl^- efflux		(Parpura and Haydon, 2009)
Histamine receptor (H_1, H_2, H_3)	Affects phospholipase C, IP_3 and Ca^{2+} release from the ER, also cAMP production	Energy metabolism, Ca^{2+} signalling	(Parpura and Haydon, 2009) (Mele and Jurič, 2013)
Hydroxycarboxylic acid receptor 1 (HCAR1)	Lactate receptor		(Ma et al., 2020)
Insulin receptor (IR)	Receptor tyrosine kinase	Energy metabolism, neuroendocrine system	(Manaserh et al., 2019)
Insulin-like growth factor 1 receptor (IGF-1)	Transmembrane receptor tyrosine kinase		(Huang et al., 2020)

Table 3 (continued).

Interferon-γ receptor (IFN-γ)	Activation of janus kinases, and signal transducer and activator of transcription proteins (Jak/Stat)		(Wang and Zhou, 2005)
Interleukin-1 receptor 1 (ILR1), interleukin-6 receptor	Activation of NF-kappa-B and MAPK pathways, signal transduction through glycoprotein 130	Epilepsy	(Ingiosi and Opp, 2016), (Quintana et al., 2013)
Kainate receptors (GluR5-GluR7, KA1, KA2)	Glutamate receptor, Na^+/K^+ channel		(Kettenmann, 2013)
Leptin receptor (LepR)	Type I cytokine receptor	Energy metabolism	(Naranjo et al., 2020)
Lysophosphatidic acid receptor (LPA)	Ca^{2+} signals, activation of MAPK and Rho pathways	Ca^{2+} signalling	(Sorensen et al., 2003)
Muscarinic cholinoreceptor (mChR M_1-M_5)	Affects phospholipase C, IP_3 and Ca^{2+} release from the ER	Ca^{2+} signalling	(Parpura and Haydon, 2009)
Natriuretic peptide receptor	Increase in cGMP		(Kettenmann, 2013)
Neurotensin receptor 2 (NTSR2)	GPCR	Epilepsy, Ca^{2+} signalling	(Kyriatzis et al., 2021)
Neurotrophin receptor (TrkB)	Receptor tyrosine kinase		(Colombo et al., 2012)
Nicotinic cholinoreceptor	$Na^+/K^+/Ca^{2+}$ channel		(Parpura and Haydon, 2009)
NMDA receptors	Glutamate receptor, $Na^+/K^+/Ca^{2+}$ channel	Ca^{2+} signalling	(Parpura and Haydon, 2009)
Opioid (γ, δ, κ, μ) receptor	Inhibits cAMP production		(Parpura and Haydon, 2009) (Nam et al., 2018)

Table 3 (continued).

Oxytocin and vasopressin receptor	Affects phospholipase C, IP_3 and Ca^{2+} release from the ER	Ca^{2+} signalling	(Parpura and Haydon, 2009)
P2X (ATP) purinoreceptor	$Na^+/K^+/Ca^{2+}$ channel	Ca^{2+} signalling, astrocyte-neuron interaction	(Parpura and Haydon, 2009)
P2Y (ATP) purinoreceptor	Affects phospholipase C, IP_3 and Ca^{2+} release from the ER	Ca^{2+} signalling	(Parpura and Haydon, 2009)
PACAP receptor (PAC_1)	Affects phospholipase C, IP_3 and Ca^{2+} release from the ER	Ca^{2+} signalling, energy metabolism	(Verkhratsky and Nedergaard, 2018)
Platelet-derived growth factor receptor α (PDGFRα)	Receptor tyrosine kinase		(Leiss et al., 2020)
Protease-activated receptor (PARs) PAR-1, PAR-2, PAR-4	GPCR	Ca^{2+} signalling	(Wang et al., 2007)
Serotonin receptor (5-HT_{1A}, 5-HT_{2A}, 5-HT_{2B}, 5-HT_4, 5-HT_{5A}, 5-HT_7)	Affects phospholipase C, IP_3 and Ca^{2+} release from the ER, also cAMP production, or triggering RhoA activity	Energy metabolism, Ca^{2+} signalling	(Parpura and Haydon, 2009) (Li et al., 2008) (Smith et al., 2011) (Müller et al., 2021)
Somatostatin receptor	Inhibition of cAMP		(Kettenmann, 2013)
Sphingosine-1-phosphate receptor (S1P)	GPCR	Ca^{2+} signalling	(Mullershausen et al., 2007)
Tachykinin receptor	Blocking K^+ and opening Cl^- channels		(Kettenmann, 2013)
Thyrotropic-releasing hormone receptor (TRH1)			(Parpura and Haydon, 2009)
Toll-like receptor (TLR)	Activates NF-κB pathway		(Chistyakov et al., 2015)

Table 3 (continued).

Trace amine-associated receptor type-1 (TAAR1)	GPCR, activation of cAMP and protein kinase A signalling		(Dave et al., 2019)
Transferrin receptor 1 (TfR1)	Involved in iron uptake by endocytosis		(Du et al., 2011)
Transforming growth factor β receptor (TGF-βR)	Serine/threonine kinase receptor	Epilepsy	(Ivens et al., 2007)
Triggering receptor expressed on myeloid cells-2 (TREM-2)	Signalling via DNAX activator proteins		(Rosciszewski et al., 2018)
Urotensin II receptor	GPCR, phospholipase C pathway and Ca^{2+} increase	Ca^{2+} signalling	(Castel et al., 2006)
Vascular endothelial growth factor receptor (VEGF)	Activates FAK and ERK		(Koyama et al., 2014)
Vasoactive intestinal polypeptide receptor (VIPR1, 2, 3)	Affects phospholipase C, IP_3 and Ca^{2+} release from the ER, also cAMP production	Energy metabolism, Ca^{2+} signalling	(Parpura and Haydon, 2009)

2.2 Modelling of Astrocyte Functions

2.2.1 Glutamate Uptake

There are a few dozen computational models, which model the effect of glutamate transporters in astrocytes or glial cells in general. These kinds of models have been published in the last few years, but they are not a completely new modelling approach (Rusakov and Kullmann, 1998). Examples of recently published studies include the studies of Tyurikova et al. (2022), Flanagan et al. (2021), Kalia et al. (2021), Héja et al. (2021), Engels et al. (2021), Armbruster et al. (2020), Borjkhani et al. (2018), Savtchenko et al. (2018), Flanagan et al. (2018), Hübel et al. (2017) and Allam et al. (2012). The study of Tyurikova

et al. was conducted using simulation tool ASTRO (Savtchenko et al., 2018), which allows the simulation of astroglial glutamate transporters. The membrane potential is calculated in the simulation, and the membrane potential landscape can be mapped on the astrocyte morphology. In the ASTRO tool, the glutamate transporter is modelled with 6 different states. The kinetics of the transporter is based on the work of Zhang et al. (2007), and the kinetic constants were adjusted to include voltage-dependency.

The study of Rusakov and Kullmann (1998) was one of the first studies that simulated the non-neuronal glutamate transporters. They modelled the transporters in the extrasynaptic space, without specifying the cell type. The theory of glutamate binding and translocation was presented with equations for glutamate concentration time course. However, the modelling was done by computing fluxes because the system had no reachable analytical solution. The simulations showed the rapid clearance of glutamate.

Allam et al. (2012) based their glutamate transporter kinetic scheme on the study of Bergles et al. (2002). A rate equation for glutamate flux was used to calculate the effect of the transporter. They showed with their simulations how the glial transporters can modulate synaptic transmission. A different research question was asked in the study of Armbruster et al. (2020). The effect of a glutamate-sensitive fluorescent reporter (iGluSnFR) on glutamate dynamics was studied with simulations. It was concluded that the indicator delays glutamate uptake because it competes with the transporters. A Markov representation was used to model the transporters. The kinetic scheme was based on the same study of Bergles et al. (2002) which Allam et al. (2012) also used, but Armbruster et al. did some simplifying modifications. The model was an extension of a previous model of Diamond (2005).

The modelling of glutamate transporters and their effects can be done using various approaches. When modelling the transport cycle, a kinetic scheme can be built, where the transporter has different states (see Figure 6). As the transporter changes from one state to another, transport substrates are moved. This corresponds to a cyclic reaction scheme with reversible reactions. The forward and backward reactions have reaction rate constants, which can be used when modelling the cycle as a Markov process or when calculating reaction rates and changes in concentrations. In biophysically and biochemically detailed models, the glutamate transporter current (the net current produced by the transporter) or the current of different ionic species (Na^+, K^+, Glu^- or H^+) can be calculated. Also, the changes in concentrations inside the cell or in the synaptic cleft can be mod-

eled, and the changes in astrocyte membrane potential can be calculated. In phenomenological models (for example Borjkhani et al. 2018), the effect of the glutamate transporter can be controlled with a single parameter, for example by reducing the input of a network. Although there are some phenomenological models, most of the models that include glutamate transport into astrocytes, are biophysical models of the synapse, including an astrocyte and a neuron or an astrocyte, a presynaptic nerve terminal and a postsynaptic neuron (the tripartite synapse). Some of these models are called multi-compartmental mathematical models considering the 3D geometry (Boucher et al., 2010; Héja et al., 2021).

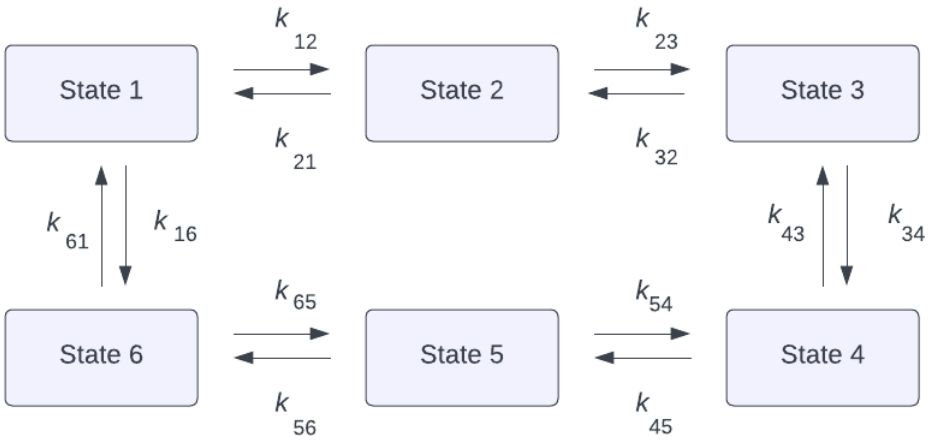

Figure 6. *Example of a kinetic scheme in the context of transporters. The cycle represents the conformational changes in one transporter molecule during the transport process. Reactions can occur in the forward direction (clockwise) or in the backward direction (counterclockwise). Each reaction is associated with a reaction rate constant k_{ij} and k_{ji}. The transport substrates associate and dissociate along the cycle (not depicted). The number of states varies depending on the transporter and the level of detail in the modelling.*

In computational modelling, the biological realism must always be kept in mind, and experimental data should be considered when building models and validating results. In the context of kinetic schemes as in Figure 6, the rate constants of reactions can be obtained based on experimental data. The glutamate transporter kinetic schemes have been developed with varying numbers of states, for example 3 (Boucher et al., 2010), 6 (Savtchenko et al., 2018), 14 (Armbruster et al., 2020; Héja et al., 2021) or 15 (Allam et al., 2012). The different numbers of states correspond to different levels of simplifications. In terms of concentrations, it is possible to treat some of the concentrations as

constant, and only model changes in certain concentrations. For example, the proton concentrations can be constant, or all the other concentrations can be constant except extracellular glutamate. In the study of Flanagan et al. (2018) only those concentrations that were low at equilibrium were modeled, and others were constant. In some studies, the glutamate itself is not of interest, but rather all the other ions that participate in the transport cycle.

The glutamate in the synaptic cleft can diffuse away or be cleared by astrocytic or neuronal glutamate transporters. In models, the astrocyte glutamate transporters can be the only mechanism that affects the extracellular glutamate concentration. Estimates can be made of the duration of a complete transport cycle. The level of detail in the transport cycle modelling varies and some models take better into account the rapid binding of extracellular glutamate and the time it takes for the transporter to release it in the intracellular side. When a Michaelis-Menten equation is used in the modelling, the half saturation constants (K_m) are not always known from experiments. The maximum uptake rate (v_{max}) can be assumed to depend on surface density of the transporter, surface area and volume, which can be used to derive the relationship between v_{max} of the neuron and the astrocyte (Hübel et al., 2017). Usually, the transporter amount is assumed to be constant, although some changes are expected to occur based on experimental data (Ibáñez et al., 2019). Assumptions can be made of the basal and peak glutamate concentrations in the synaptic cleft, for example 0 and 1 mM concentrations can be assumed for basal and peak values, but there is variation between different models.

2.2.2 Calcium Signalling

Modelling of astrocyte functions has largely focused on the role of Ca^{2+} signaling. Many of these models focus on the role of IP_3-dependent Ca^{2+} release from the endoplasmic reticulum. An extensive review of these Ca^{2+} models of astrocytes has been made by Manninen et al. (2018). For example, single astrocyte models are listed in Table 2 of that review. Interestingly, it was found in the review that many of the models were quite similar, originating from a few previous modelling studies.

One possible simulator for biochemical reactions with 3D morphologies of the cells is STEPS (Stochastic Engine for Pathway Simulation) (Hepburn et al., 2012). It allows the simulation of reaction-diffusion systems. STEPS was used in the study by Denizot et al.

(2019), which simulated Ca^{2+} dynamics and the effect of spatial organization of IP_3R. Their simulation results were produced in morphologies mimicking the fine astrocyte processes. The results indicated that differences in IP_3R localization could be the source of variation in the observed Ca^{2+} signals. The ASTRO simulation tool (Savtchenko et al., 2018) can be used to study calcium signalling as well. With ASTRO, it has been shown how changes in Ca^{2+} buffering can affect the Ca^{2+} waves (Savtchenko et al., 2018).

3. OBJECTIVES

In this thesis, the objective is to study glutamate transport in astrocytes using a biophysically detailed single-cell computational model which includes detailed descriptions of the cellular functions of interest. The first aim is to study the kinetics of glutamate transport which means the temporal behaviour of the transport process and the generated ion concentrations and ionic currents. The second aim is to study whether a Ca^{2+} signal is associated with the transport process. The third aim is to study the model behaviour which means studying how the model handles different initial conditions. In summary, with these simulations, it is possible to study astrocyte glutamate transporter function and get validation for existing hypotheses related to these transporters and their physiology.

4. MATERIALS AND METHODS

4.1 ASTRO Simulation Tool

ASTRO is a simulation tool for studying morphology-based astrocyte physiology. It was presented in 2018 by Savtchenko et al. The simulation tool utilises MATLAB and NEURON for building the cell morphology and 3D structure, and NEURON for creating the simulations (see Figure 7). The NEURON simulation environment is presented in Section 4.2. Several astrocyte membrane mechanisms are available for simulation in the ASTRO tool. The user is also able to add new mechanisms if needed. In the above literature review, tables of different astrocyte channels, transporters, and receptors were presented (Table 1, Table 2, Table 3). It is worth noting that only a very small fraction of these is available in the simulator. Some mechanisms are more universal and expressed in astrocytes throughout different brain regions, and consequently can be considered as the most essential ones. However, the computational neuroscience community should keep in mind the variety of mechanisms that exist and which can possibly contribute to and explain some phenomena. This will be relevant in the future when more brain-area specific knowledge is available.

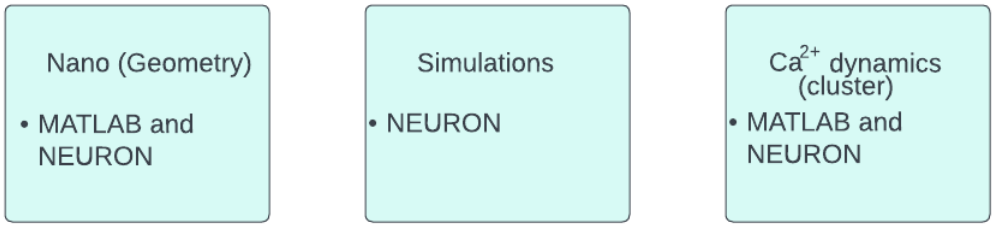

Figure 7. *The modules of ASTRO. The main software that is used in each module is also shown. The first module is for building the morphology, the second is for biophysical simulations and the third is for Ca^{2+} simulations that require a computer cluster.*

The mechanisms that are available in ASTRO are mostly well-known and accepted mechanisms of astrocytes. Passive mechanisms (named pas in ASTRO) include the channels that set up the membrane potential of astrocytes and do not need any activation to be open for current flow. Other channel mechanisms include the inwardly rectifying K^+ channel, which is available in two forms (Kir4 and Kir). The delayed rectifier K^+ channel

is also implemented (kdrglia). Gap junction mechanisms exist in three forms (gap junction, gapCa, gapCaSt) and Ca^{2+} channel is also available (L-type Ca^{2+} channel). Gap junction describes generally a current through gap junctions, while gapCa and gapCaSt describe Ca^{2+} current through gap junctions. Two cell membrane pumps (kpump and Ca^{2+} pump) and one transporter (GluTrans) can be used. The K^+ pump (kpump) is implemented to only pump K^+, but assumably the biological counterpart is the Na^+/K^+-ATPase, and Na^+ is not modelled.

Some mechanisms are developed by Savtchenko et al. (2018) themselves, and some they have taken for example from ModelDB, a database for neuronal models (McDougal et al. 2017, https://senselab.med.yale.edu/ModelDB/). The mechanisms described here are only the cell membrane mechanisms, but additional mechanisms are available in ASTRO, most importantly the ER Ca^{2+} dynamics. The users must pay attention to understanding which mechanisms are in use when they do simulations. It is also important to understand how the mechanisms interact. For example, if one mechanism affects concentrations of ions, do the other mechanisms see this change or not.

There are different simulations available to be performed on the specified morphology. One of them is a fluorescence recovery after photobleaching (FRAP) simulation, which assesses the diffusion and connectivity properties. The electrophysiological properties can be simulated for example by looking at the voltage responses to current injections. Regarding physiological processes, simulations for Ca^{2+} dynamics, glutamate transporter function and K^+ dynamics can be done.

4.2 NEURON Simulation Environment

NEURON simulator is built to enable the study of biophysical models of single neurons and networks of neurons (Carnevale, 2006). It is widely used in computational neuroscience field. The benefits of using a simulator instead of a custom code are the comparability of models, intuitive syntax, and available support. For example, NEURON forum is a place for discussion and the developers provide answers for questions that the users may have (NEURON, 2020). During the model setup, user specifies the neuron morphology and biophysical properties. Graphical user interface tools are available for building the model, but the mechanisms can also be described using NMODL model description language. Users can share their NMODL code files for example in ModelDB.

The fundamental equation in NEURON is the discrete form of the cable equation. This equation describes the conservation of charge. It states that the capacitive current plus the membrane current that leaves a compartment must equal the current that enters from adjacent compartments (Carnevale, 2006):

$$C_m \frac{dV_m}{dt} + i_{ion} = \sum i_a \ , \quad (1)$$

where C_m is the membrane capacitance, V_m is the membrane potential, t is time, i_{ion} is the current flowing through the membrane and i_a is the axial current from neighbouring compartments. It is important to recognize the sign conventions of different currents. The current that is generated by positive ions moving from the inside to the outside of the cell has a positive sign, and the same is true for the current that is coming into a compartment from adjacent regions. In NEURON, the morphology is built from sections that are connected to each other. Section is a piece of cable which is unbranched. A parameter called *nseg* determines how many points are included in one section. These are the points where Equation 1, the discrete cable equation, is integrated to get the value of membrane potential.

4.3 Adding Mechanisms to ASTRO/NEURON

New mechanisms for the NEURON simulation environment can be written with NMODL model description language. NMODL is a high-level language, which aims to provide clear syntax for specifying models. The statements get translated to C language. The code file is divided into predetermined blocks, and the usage of each block is explained in the user manual. The mechanism of interest is described with equations (differential and algebraic). Alternatively, chemical reactions can also be intuitively written by using a kinetic block.

In this work the goal was to simulate glutamate transporter function in a biophysical astrocyte model. Additionally, the link between glutamate transporter function and Ca^{2+} signal is of interest. The ASTRO simulator has an existing glutamate transporter model which can be used to simulate the response when glutamate is applied to a certain area of the cell. The response is monitored by looking at extracellular glutamate concentration and the current injected into the cell in a voltage clamp configuration. However, the existing simulation was not suitable for the purpose of this work, because the simulation was intended to only study the transporter current. In this work, the purpose was to study

the glutamate uptake kinetics in a way that would utilize chemical reaction kinetics to get the concentrations of different ions. A custom glutamate transporter simulation was built to study the research questions of interest. The complete code for this is presented in Appendix. To study the Ca^{2+} signal generated by NCX in response to glutamate transport, an already available model code was used (Hay et al. 2011, Zylbertal et al. 2017, available in ModelDB under accession number 230326). This NCX code was kept unchanged except for two slight modifications: 1) the mechanism also affects Na^{+} current, and 2) the Ca^{2+} current is -1x rate instead of -2x rate.

The kinetic scheme of glutamate transporter function is based on the work of Zhang et al. (2007). Some of the modelling choices were kept similar as in the built-in glutamate transporter simulation, for example the amount of transporters (in mol/cm^2), initial ion concentrations and the total charge transported in one cycle. The main equations are explained below:

$$State1 + [Glutamate]_o \leftrightarrow State2\ (k_{12}u(V_m, -0.1), k_{21}u(V_m, 0.1)) \quad (2)$$

$$State2 + [Na^+]_o \leftrightarrow State3\ (k_{23}u(V_m, 0.5), k_{32}u(V_m, -0.5)) \quad (3)$$

$$State3 \leftrightarrow State4\ (k_{34}u(V_m, 0.4), k_{43}u(V_m, -0.4)) \quad (4)$$

$$State4 \leftrightarrow State5 + [Glutamate]_i\ (k_{45}, k_{54}) \quad (5)$$

$$State5 \leftrightarrow State6 + [Na^+]_i\ (k_{56}u(V_m, 0.6), k_{65}u(V_m, -0.6)) \quad (6)$$

$$State6 + [K^+]_i \leftrightarrow State1 + [K^+]_o\ (k_{61}u(V_m, 0.6), k_{16}u(V_m, -0.6)), \quad (7)$$

where state is the conformational state of the transporter, k_{ij} and k_{ji} are the rate constants for forward and backward reactions and $u(V_m, z)$ is a voltage-dependence equation for the rate constants. The voltage-dependence equation is the following (Reynolds et al., 1985):

$$u(V_m, z) = e^{\left(\frac{-zFV_m}{2RT}\right)}, \quad (8)$$

where V_m is voltage, z is the number of charges moved in the reaction under consideration, F is the Faraday constant, R is the gas constant and T is the temperature.

The transporter has 6 conformations in this kinetic scheme, and based on Equations 2-7, the differential equations representing the change in transporter conformations are the following:

$$\frac{d\,[State1]}{dt} = -k_{12}[State1][Glu]_o u(V_m, -0.1) + k_{21}[State2]\, u(V_m, 0.1) - k_{16}[State1][K]_o u(V_m, -0.6) + k_{61}[State6][K]_i u(V_m, 0.6) \quad (9)$$

$$\frac{d\,[State2]}{dt} = -k_{23}[State2][Na]_o u(V_m, 0.5) + k_{32}[State3]u(V_m, -0.5) - k_{21}[State2]u(V_m, 0.1) + k_{12}[State1][Glu]_o u(V_m, -0.1) \quad (10)$$

$$\frac{d\,[State3]}{dt} = -k_{34}[State3]u(V_m, 0.4) + k_{43}[State4]u(V_m, -0.4) - k_{32}[State3]u(V_m, -0.5) + k_{23}[State2][Na]_o u(V_m, 0.5) \quad (11)$$

$$\frac{d\,[State4]}{dt} = -k_{45}[State4] + k_{54}[State5][Glu]_i - k_{43}[State4]u(V_m, -0.4) + k_{34}[State3]u(V_m, 0.4) \quad (12)$$

$$\frac{d\,[State5]}{dt} = -k_{56}[State5]u(V_m, 0.6) + k_{65}[State6][Na]_i u(V_m, -0.6) - k_{54}[State5][Glu]_i + k_{45}[State4] \quad (13)$$

$$\frac{d\,[State6]}{dt} = -k_{61}[State6][K]_i u(V_m, 0.6) + k_{16}[State1][K]_o u(V_m, -0.6) - k_{65}[State6][Na]_i u(V_m, -0.6) + k_{56}[State5]u(V_m, 0.6). \quad (14)$$

Based on the kinetic scheme that is written to the kinetic block of the model code file, NEURON automatically assigns values to variables *f_flux and b_flux* (forward and backward flux) during the simulation. To calculate the current that is generated by different ions, the net flux value (forward flux minus backward flux) must be then multiplied by Faraday's constant. The transporter moves 3 Na^+ ions and 1 glutamate molecule into the cell, and 1 K^+ ion out of the cell. Because in this scheme there are three different ions moving, both inside and outside of the cell, the sign convention must be considered when calculating the current values. This means marking positive ions moving out of the cell as positive current, and positive ions moving into the cell as negative current. Also, in the case of Na^+, the current must be multiplied by three, because in the scheme only one Na^+ ion is moving while the true number is three, meaning that the actual current for Na^+ is three times the one that is resulting from the scheme.

In addition to the above-described glutamate transporter model, a few alternative models were implemented and tested. One of them is based on the work of Bergles et al. (2002) and it is compared in this study with the final model that is based on the work of Zhang et al. (2007). The equations that describe the alternative model are:

$$State1 + [Na^+]_o \leftrightarrow State2\ (k_{1f}\, u(V_m, 0.46), k_{1b} u(V_m, -0.46)) \quad (15)$$

$$State2 + [Na^+]_o \leftrightarrow State3\ (k_{2f}, k_{2b}) \quad (16)$$

$$State3 + [H^+]_o \leftrightarrow State4\ (k_{3f}, k_{3b}) \quad (17)$$

$$State4 + [Glu]_o \leftrightarrow State5\ (k_{4f}, k_{4b}) \quad (18)$$

$$State5 + [Na^+]_o \leftrightarrow State6\ (k_{5f}u(V_m, 0.55), k_{5b}u(V_m, -0.55)) \quad (19)$$

$$State6 \leftrightarrow State7\ (k_{6f}, k_{6b}) \quad (20)$$

$$State7 \leftrightarrow State8 + [Na^+]_i\ (k_{7f}u(V_m, 0.04), k_{7b}u(V_m, -0.36)) \quad (21)$$

$$State8 \leftrightarrow State9 + [H^+]_i\ (k_{8f}, k_{8b}) \quad (22)$$

$$State9 \leftrightarrow State10 + [Glu]_i\ (k_{9f}, k_{9b}) \quad (23)$$

$$State10 \leftrightarrow State11 + [Na^+]_i\ (k_{10f}, k_{10b}) \quad (24)$$

$$State11 \leftrightarrow State12 + [Na^+]_i\ (k_{11f}, k_{11b}) \quad (25)$$

$$State12 + [K^+]_i \leftrightarrow State13\ (k_{12f}, k_{12b}) \quad (26)$$

$$State13 \leftrightarrow State14\ (k_{13f}u(V_m, 0.531), k_{13b}u(V_m, -0.059)) \quad (27)$$

$$State14 \leftrightarrow State1 + [K^+]_o\ (k_{14f}, k_{14b}), \quad (28)$$

where state is the conformational state of the transporter, k_f and k_b are the rate constants for forward and backward reactions and $u(V_m, z)$ is a voltage-dependence equation for the rate constants (Equation 8).

The outcomes of these simulations will be concentration values, current density values and whole-cell currents in voltage clamp configuration. Current density is the current divided by area (mA/cm^2). The voltage clamp simulation simulates an experiment where the membrane potential of the cell is kept constant by injecting current to the soma, and this makes it possible to infer the currents that are flowing through the membrane.

4.4 Modelling Passive Properties

The modelling of astrocyte passive properties can be done similarly as is done for neurons. The resting membrane potential, the potential difference between inside and outside of the cell, is formed by so-called leak ion channels. The leak ion channels are ion channels which have linear current-voltage relationships (so-called I-V relationships), and they allow the current flow without the need for channel activation. This is contrary to voltage-gated ion channels, which have non-linear I-V characteristics and are activated by changes in membrane potential.

The cell membrane and ion channels are typically considered as an equivalent electrical circuit in computational neuroscience. The electrochemical gradient corresponds to a

battery, ion channels to resistors, and the cell membrane to a capacitor. The charge stored on a capacitor is:

$$q = CU, \tag{29}$$

where *C* is the capacitance and *U* is the voltage (Koch, 1999). The electrochemical gradient is the driving force for the movement of ions. Equilibrium potential is the potential difference when no net movement of a given ion is occurring. This means that when the membrane potential is not the same as the equilibrium potential for an ion, the ion moves in the direction which drives the membrane potential closer to the equilibrium potential for that ion. Equilibrium potentials can be calculated using the Nernst equation:

$$E = \frac{RT}{zF} \ln \frac{[ion]_{in}}{[ion]_{out}}, \tag{30}$$

where *R* is the gas constant, *T* is the temperature in kelvins, *z* is the valency of the ion, *F* is Faraday's constant and $[ion]_{in}$ and $[ion]_{out}$ are the intracellular and extracellular concentrations of the ion (Sterratt et al., 2011).

The ionic currents are often described using the Ohm's law (Koch, 1999):

$$I = \frac{U}{R}, \tag{31}$$

where *U* is the voltage and *R* is the resistance. In the context of ion channels, the current is written as:

$$I = g(V_m - E), \tag{32}$$

where *g* is the conductance (1/*R*), V_m is the membrane potential and *E* is the equilibrium potential. This describes the current that is flowing through a particular ion channel type. The currents affect the membrane potential, and this is described as:

$$\frac{dV_m}{dt} = \frac{I}{C}, \tag{33}$$

where *I* is the current and *C* is the capacitance. Equation 33 results from Equation 29.

In a passive compartmental model, in addition to the leak current through ion channels, it is possible to consider the current that flows passively from neighbouring regions. For this purpose, the following expression can be considered:

$$I = \frac{d}{4R_a} \frac{\partial^2 V_m}{\partial x^2}, \tag{34}$$

where *d* is the diameter, R_a is the axial resistivity, V_m is the membrane potential and *x* is the distance. The resulting equation for membrane potential in a passive model thus includes the currents that result from the leak channels and the spread of current between different regions of the cell:

$$C_m \frac{\partial V_m}{\partial t} = -\overline{g_L}(V_m - E_L) + \frac{d}{4R_a} \frac{\partial^2 V_m}{\partial x^2}, \tag{35}$$

where C_m is the specific membrane capacitance, t is time, $\overline{g_L}$ is leak current conductance and E_L is the equilibrium potential for the leak current (Sterratt et al., 2011).

5. RESULTS AND DISCUSSION

5.1 Comparing Two Glutamate Transporter Models

This thesis work first involved review and qualitative analysis of glutamate transporter models available in the literature (manuscript in preparation). A few alternative, biophysically detailed glutamate transporter models were then selected and tested to find the most suitable ones. In this section, the final selected model (Model 1) is compared to one other alternative (Model 2) to justify why Model 1 was chosen. The modelling principle was the same in these two models, and the main difference was the number of states that described the transport cycle and the values of kinetic constants. Model 1 is based on the kinetic scheme of Zhang et al. (2007) and has 6 states. Model 2 is based on the kinetic scheme of Bergles et al. (2002) and has 14 states. In the following simulations, different ion concentrations and currents are simulated.

The models were tested in a situation, where the transporter is in steady state, and ion concentrations are at physiological, resting levels. The extracellular glutamate concentration was then raised to 0.5 mM and the response was simulated in one process of the astrocyte morphology. The responses of the models regarding concentration changes can be seen in Figures 8–11.

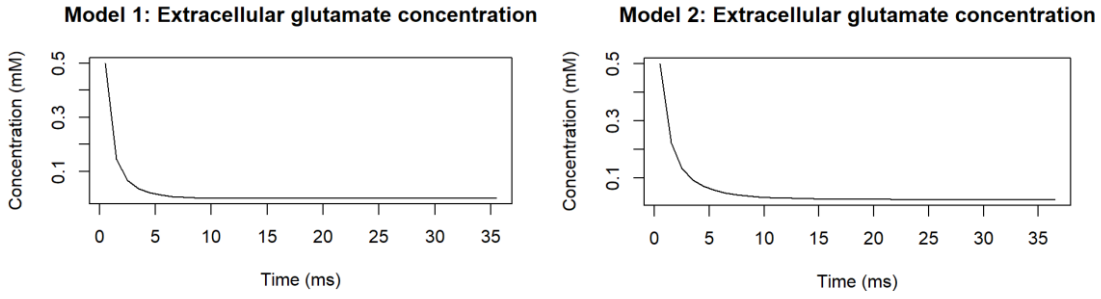

Figure 8. *Extracellular glutamate concentration in response to glutamate transporter function in two different models.*

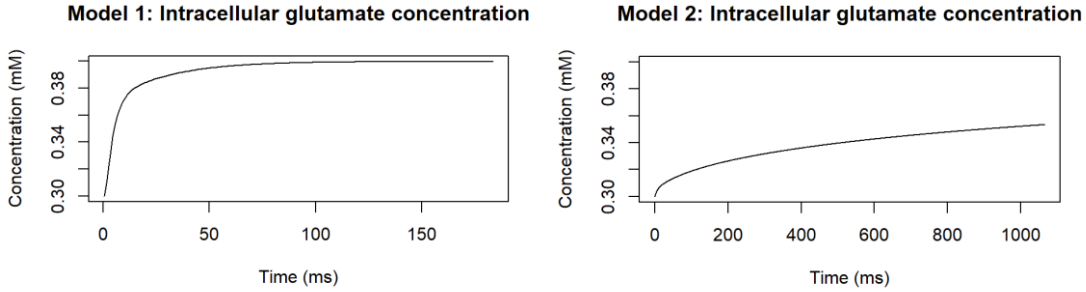

Figure 9. *Intracellular glutamate concentration in response to glutamate transporter function in two different models. Note the different x-axis scale.*

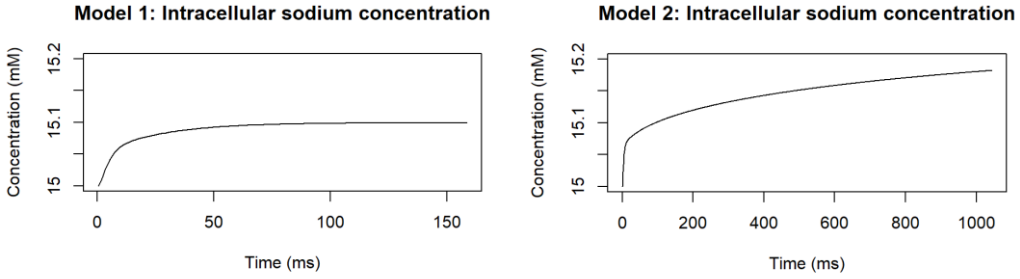

Figure 10. *Intracellular Na^+ concentration in response to glutamate transporter function in two different models. Note the different x-axis scale.*

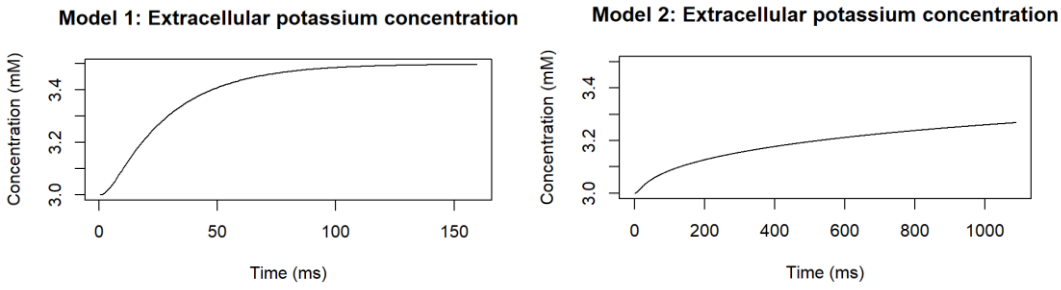

Figure 11. *Extracellular K^+ concentration in response to glutamate transporter function in two different models. Note the different x-axis scale.*

As can be seen in Figures 8-11, there are some clear differences in the model behaviours, although the concentration curves of glutamate, K^+ and Na^+ resemble each other in shape. The most obvious difference is that Model 2 operates on a much slower time scale. The simulations were stopped by 1100 ms at the latest, and Model 2 did not reach

the steady-state values in that time in most cases. Contrary to Model 2, Model 1 operates on a relatively fast time scale, and reaches final values in tens of milliseconds. Both models produce outputs which resemble logarithmic functions, where changes happen more quickly in the beginning and then slow down. An interesting finding is that both models also clear the extracellular glutamate very quickly, in less than 10 ms, although in the case of Model 2, the concentration does not go exactly to zero. The rapid clearance of extracellular glutamate is a good indication, because the transporter is thought to bind the extracellular glutamate very fast, after which the translocation steps to the cytosol would take a little bit more time (Grewer et al., 2000). This behaviour is seen in both models, but with a large difference in the translocation time between the two models.

The time scale of Model 1 is more in line with previous studies (Diamond, 2005). It may be speculated that the 14-state Model 2, with those kinetic constants, is too slow. In the 1100 ms time, Model 2 does not reach as high concentration values of intracellular glutamate and extracellular K^+ as Model 1, but the intracellular Na^+ concentration is higher than in Model 1. This is probably because Model 2 has more accurate representation of the transport cycle regarding Na^+ and incorporates the binding of 3 Na^+ ions in separate reactions. In Model 1, only one Na^+ binding reaction is incorporated, which is one downside of the model. It may be assumed that the intracellular Na^+ concentration that results from Model 1 is slightly too low.

In addition to the concentration responses, the currents produced by the transporter function were compared between the two models. Two different measures were examined: the current density in one astrocyte process (Figure 12) and the whole cell current measured in voltage clamp configuration at the soma (Figure 13).

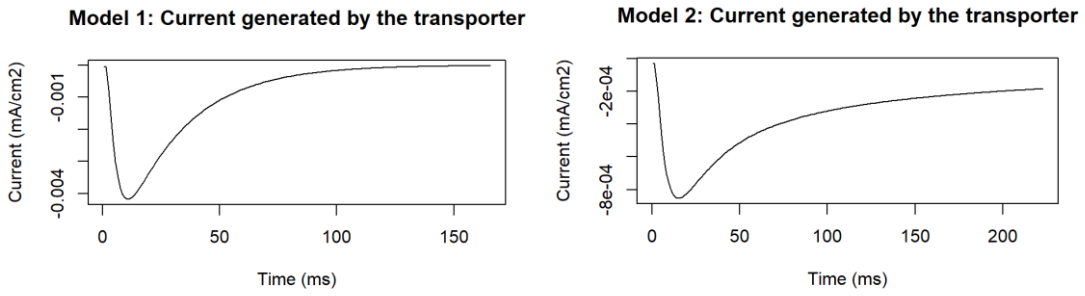

Figure 12. *Current density of glutamate transporters in two different models. Note the different x- and y-axis scales.*

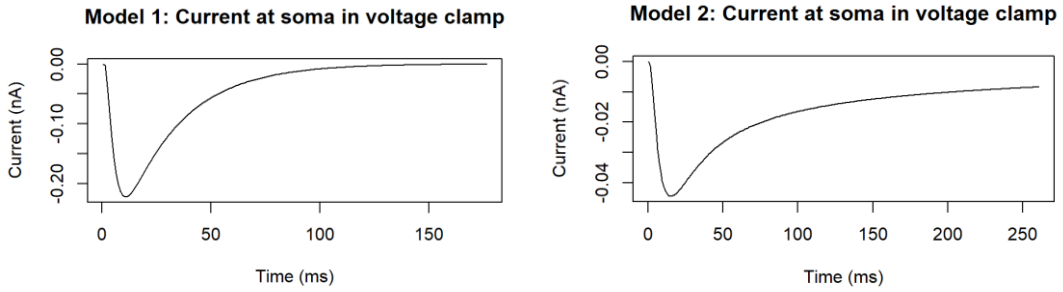

Figure 13. *Voltage clamp at soma in response to glutamate transporter function in two different models. Note the different x- and y-axis scales.*

As can be seen in Figures 12 and 13, Model 1 produces a larger current, with an amplitude close to 0.25 nA in voltage clamp. The current of Model 1 goes back to zero, while the current in Model 2 stays below zero for a longer period. The shape of the curve in Model 1 seems to be closer to experimental findings than the shape produced by Model 2 (Diamond, 2005). Glutamate transporter currents have been studied previously both experimentally and computationally. These studies have produced varying results, but based on them, the current responses of the two models seem to be in the correct scale regarding the amplitude. Previous studies include those of Diamond et al. (1998), Diamond (2005), Zhang et al. (2009), Unichenko et al. (2012), Afzalov et al. (2013), Campbell et al. (2014) and Wanke et al. (2016). For example, in the study of Diamond (2005), the amplitude of the transporter current was close to 0.15 nA and the response lasted around 40 ms as estimated from Figure 1 of that study. These values are relatively close to those produced by Model 1. Factors that influence these current values include glutamate transporter density and the stimulus magnitude (extracellular glutamate concentration). Based on the results presented above, Model 1 was selected as the most promising model, and it was used in further analyses.

5.2 Studying the Effect of Glutamate Transporters on NCX

The interesting research question to be tested was whether glutamate transporter function can induce a Ca^{2+} signal. There is some evidence showing that NCX can generate Ca^{2+} signals in response to the uptake of glutamate (Ibáñez et al., 2019; Kirischuk et al., 2007; Oschmann et al., 2017; Rojas et al., 2007). The hypothesis behind this is that the Na^{+} accumulation in the close vicinity of the intracellular side of the cell membrane reverses NCX function. This would result in Na^{+} being transported out of the cell, and Ca^{2+}

being transported into the cell by NCX. The interplay between glutamate transporters and NCX was tested with Model 1, in response to 0.5 mM extracellular glutamate concentration. The Na^+ and Ca^{2+} currents of NCX are shown when there are no glutamate transporters (Figure 14) and when the transporters are present (Figure 15), to see the effect of the transporters.

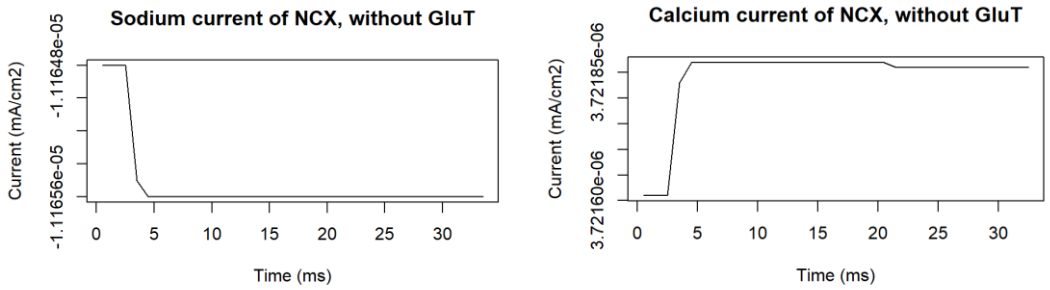

Figure 14. *Na^+ and Ca^{2+} currents of NCX when there are no glutamate transporters (GluT).*

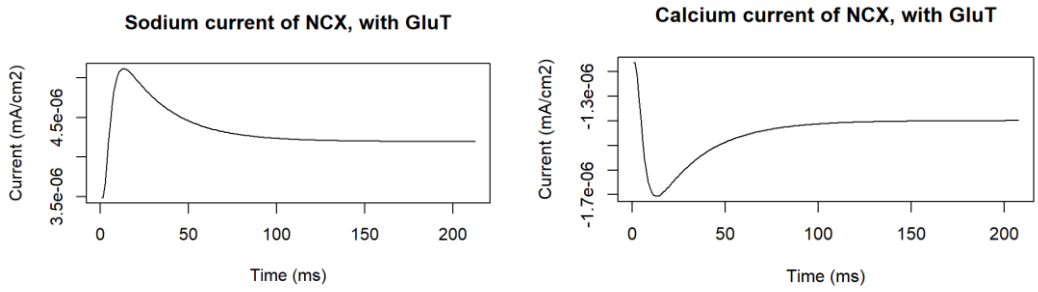

Figure 15. *Na^+ and Ca^{2+} currents of NCX when the glutamate transporters (GluT) are functional.*

The results show that glutamate transporters reverse the NCX function. Without transporters (Figure 14), the Na^+ current is negative (current into the cell) and Ca^{2+} current is positive (current out of the cell). When the transporters are added to the model (Figure 15), both Na^+ and Ca^{2+} currents reverse their sign and direction, indicating that Ca^{2+} enters the cell, creating a Ca^{2+} signal. The currents seem to be relatively small, and it would be interesting to know whether they are relevant to the cell function. In one study, long reverse operation of NCX (>20 s) was needed to activate the CICR mechanism of the cell, which amplifies the Ca^{2+} signal (Rojas et al., 2007). It could be hypothesized

that these types of longer periods of reverse operation of NCX could happen in prolonged neuronal activation when glutamate is released repeatedly to the synaptic cleft. Whether the shorter period of NCX activity and the resulting smaller Ca^{2+} signal has a physiological consequence remains unknown. Overall, these results support the hypothesis that a Ca^{2+} signal is generated in response to glutamate transporter function, although more research on this subject is needed.

5.3 Additional Testing of the Glutamate Transporter Model

The glutamate transporter model was additionally tested to see the model behaviour in various conditions. First, it was tested how the model behaves when the input (extracellular glutamate concentration) is significantly higher (1 mM) or lower (0.1 mM) than in the previous tests (0.5 mM). The results can be seen in Figure 16.

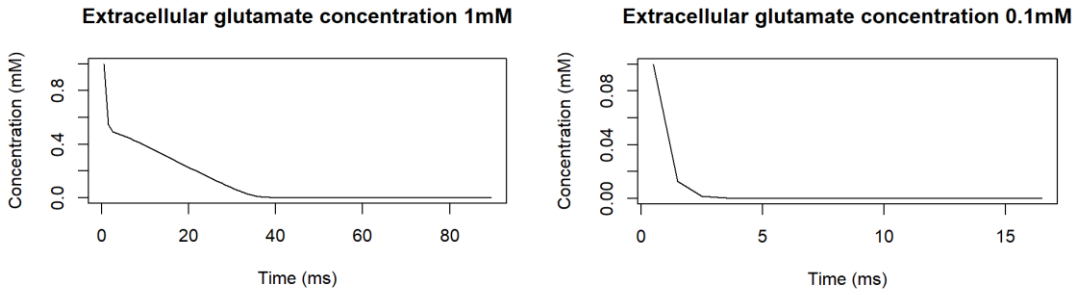

Figure 16. *Extracellular glutamate concentration changes due to transporter function, with different starting concentrations (1mM, left, and 0.1 mM, right). Note the different x- and y-axis scales.*

The results show that clearing 1 mM of glutamate takes slightly longer and clearing 0.1 mM of glutamate takes slightly less time than the original model with 0.5 mM starting concentration, as expected. However, the difference between the original 0.5 mM concentration and the 1 mM concentration was rather significant. The concentration of 0.5 mM was cleared in about 5 ms, whereas it took almost 40 ms to clear 1 mM glutamate concentration. This indicates that with certain extracellular glutamate concentration range, at least from 0.1 mM to 0.5 mM based on these results, the uptake is very fast and happens in milliseconds. Higher values will quite significantly slow down the uptake process in this model. If the glutamate uptake slows down, the prolonged high extracellular glutamate concentration could contribute to neurotoxicity.

The second test was to see whether moderate changes of other ion concentrations affect the uptake capacity of the model. Intracellular Na^+ concentration was raised from 15 mM to 20 mM (Figure 17).

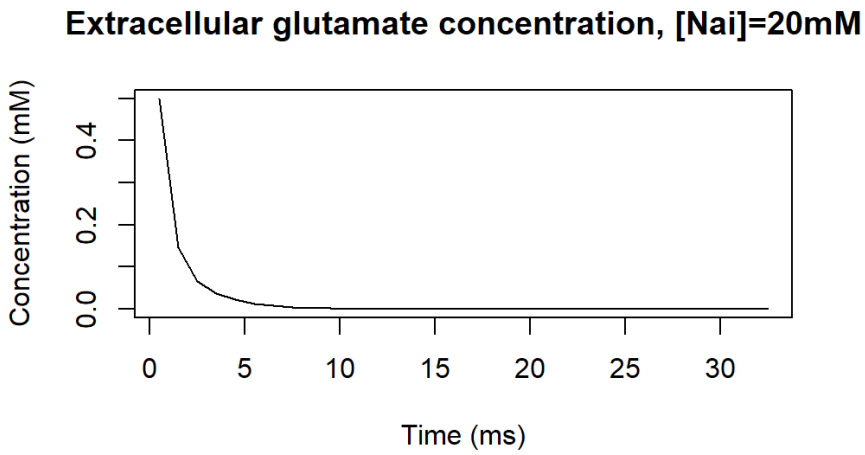

Figure 17. *Extracellular glutamate concentration when intracellular Na^+ concentration is raised to 20 mM.*

It seems that moderate changes in ion concentrations do not have any effect on the uptake capacity of glutamate. This would indicate that the system is not easily affected by concentration changes, and it maintains the ability to quickly uptake glutamate. It would be expected that larger changes influence the uptake capacity, because the uptake relies on the concentration gradient of ions.

The last experiment was to test different transporter amounts. The original concentration of 1.66×10^{-12} mol/cm^2 was modified to be either one tenth (10%) of original or 70% of original, to see how either a large or a small reduction affects the function. The results can be seen in Figure 18.

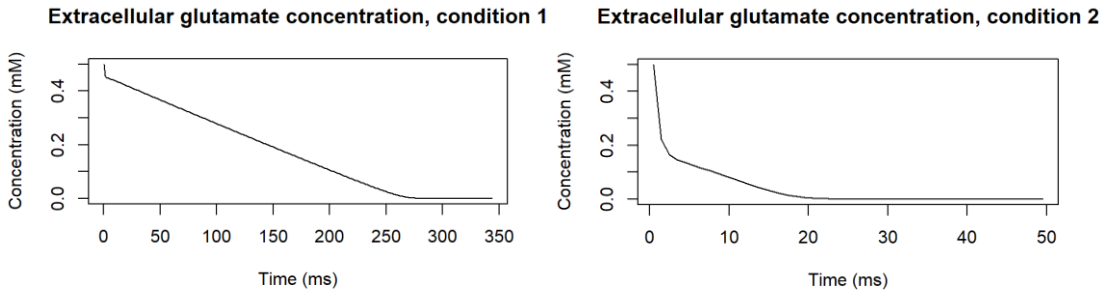

Figure 18. *Extracellular glutamate concentration when transporter amount is 10% of original (condition 1) and 70% of original (condition 2).*

From these results, it can be concluded that the transporter amount is a key parameter, which affects the results. With 10% of original transporter amount (condition 1), the transport process takes around 250–300 ms. When the transporter concentration was 70% of original (condition 2), the glutamate uptake time increased from about 5 ms to about 20 ms. This indicates that fluctuations in transporter amount, which can happen through transporter internalization and re-positioning to the membrane, are relevant for the uptake time of glutamate. If this is the case, it would be interesting to study transporter amount and the factors influencing it in more detail. This could be further analysed in experimental studies. The simulations presented in this study are an example of the usefulness of computational modelling – they provide ideas and hypotheses to be tested experimentally. Additionally, because there is not a lot of experimental data on the glutamate uptake details available, computational modelling is an important approach which provides new information. In the future experimental studies, these dynamic interactions between different mechanisms can be studied in more detail.

6. CONCLUSIONS

Astrocytes have many functions in the central nervous system. They control homeostasis of ions and neurotransmitters, energy metabolism and vascular function, and they seem to participate in information processing in the brain as well (Haim and Rowitch, 2017). In this thesis the specific interest was to study astrocyte glutamate transport which is a fundamental process that enables normal neurotransmission by controlling the synaptic glutamate concentration. Disruptions in glutamate transport have consequences which may lead to various diseases.

To study glutamate transporters with a computational model, ASTRO was chosen as the simulation tool because it is specifically made for studying biophysical properties of astrocytes and provides some important features making the modelling easier when everything does not need to be made from the scratch. One type of glutamate transport simulation already existed in the simulator, but a custom model was implemented for the purpose of this work, to enable studying the specific research questions of interest.

Multiple previously published models were first qualitatively analysed and their implementations were tested for the glutamate transporter simulations. At the end, two of them, the models by Zhang et al. (2007) and Bergles et al. (2002), were selected for final comparison and simulations in this work. Both had some promising features, but the model by Zhang et al. (2007) was chosen for further analysis because it operated considerably faster than the other one, which was a desired property. Importantly, the glutamate uptake time was closer to the experimental findings. The model by Zhang et al. (2007) cleared extracellular glutamate of 0.5 mM concentration very quickly, in about 5 ms. The current amplitude in voltage clamp configuration was about 0.25 nA, which seemed to be in the correct range based on previous studies (Diamond, 2005). The shape of the current curve was also similar to what was expected, and the current lasted for about 50 ms.

One central question that was tested with the model by Zhang et al. (2007) was whether a Ca^{2+} signal is generated in astrocytes in response to glutamate transporter function. For this purpose, NCX was added to the simulations, because it is hypothesised that this exchanger could generate a Ca^{2+} signal after the activation of glutamate transporters. The NCX function was simulated both when there were no glutamate transporters present and when they were present. It was found that NCX reverses its operation in the

presence of glutamate transport, meaning that a Ca^{2+} signal is generated. This is one indication for the association of glutamate transport function and Ca^{2+} signal, but the possible consequences of the signal remain to be studied. Furthermore, it is not known whether a small Ca^{2+} signal is relevant, or if a longer period of NCX reverse operation is required to generate a response in the cell. The predictions given by the model could be used as a starting point to design new experiments.

Further analyses of the glutamate transporter model revealed that while the model is fast in clearing 0.5 mM glutamate, it takes significantly longer to clear the extracellular glutamate which is twice as high (1 mM). The uptake time rose from about 5 ms to almost 40 ms. Moderate changes in concentrations of other ions relevant for the transport did not affect the uptake capacity. The transporter amount is a key parameter defining the time course of glutamate uptake. When the transporter amount was 70% of original, the uptake time increased from 5 ms to about 20 ms with 0.5 mM glutamate concentration. Because transporter amount in the cell membrane is known to vary, these results predict that the synaptic glutamate concentration may be significantly different depending on how many transporters are currently internalized or inserted to the membrane.

In this work, glutamate transporters and Na^{+}-Ca^{2+} exchangers were modelled in the ASTRO simulator. Insights of the transporter function regarding time scales, concentration changes and currents are provided, in addition to test results for different conditions including initial glutamate concentration in the synaptic cleft and transporter concentration. The computational model provided validation to the Ca^{2+} signal hypothesis that has been seen in some experiments. On the other hand, the model also produced some results that could inspire some experimental work. Ideally, computational models and experimental work benefit from each other, advancing developments in neuroscience.

REFERENCES

Abbott, N.J., Pichon, Y., 1976. Mechanisms for the passive regulation of extracellular K+ in the central nervous system: the implications of invertebrate studies. Advances in experimental medicine and biology, Advances in Experimental Medicine and Biology 69, 151–164. https://doi.org/10.1007/978-1-4684-3264-0_12.

Acaz-Fonseca, E., Avila-Rodriguez, M., Garcia-Segura, L.M., Barreto, G.E., 2016. Regulation of astroglia by gonadal steroid hormones under physiological and pathological conditions. Progress in Neurobiology, Targeting Astrocytes in Brain Injuries: A Translational Research Approach 144, 5–26. https://doi.org/10.1016/j.pneurobio.2016.06.002.

Afzalov, R., Pryazhnikov, E., Shih, P.-Y., Kondratskaya, E., Zobova, S., Leino, S., Salminen, O., Khiroug, L., Semyanov, A., 2013. Low micromolar Ba^{2+} potentiates glutamate transporter current in hippocampal astrocytes. Frontiers in Cellular Neuroscience 7. https://doi.org/10.3389/fncel.2013.00135.

Allam, S., Ghaderi, V., Bouteiller, J.-M., Legendre, A., Nicolas, A., Greget, R., Bischoff, S., Baudry, M., Berger, T., 2012. A Computational model to investigate astrocytic glutamate uptake influence on synaptic transmission and neuronal spiking. Frontiers in Computational Neuroscience 6. https://doi.org/10.3389/fncom.2012.00070.

Andersen, J.V., Schousboe, A., Verkhratsky, A., 2022. Astrocyte energy and neurotransmitter metabolism in Alzheimer's disease: Integration of the glutamate/GABA-glutamine cycle. Progress in Neurobiology 217, 102331. https://doi.org/10.1016/j.pneurobio.2022.102331.

Araque, A., Parpura, V., Sanzgiri, R.P., Haydon, P.G., 1999. Tripartite synapses: glia, the unacknowledged partner. Trends in Neurosciences 22, 208–215. https://doi.org/10.1016/S0166-2236(98)01349-6.

Armbruster, M., Dulla, C.G., Diamond, J.S., 2020. Effects of fluorescent glutamate indicators on neurotransmitter diffusion and uptake. eLife 9, e54441. https://doi.org/10.7554/eLife.54441.

Armbruster, M., Naskar, S., Garcia, J.P., Sommer, M., Kim, E., Adam, Y., Haydon, P.G., Boyden, E.S., Cohen, A.E., Dulla, C.G., 2022. Neuronal activity drives pathway-specific depolarization of peripheral astrocyte processes. Nature Neuroscience 25, 607–616. https://doi.org/10.1038/s41593-022-01049-x.

Aronica, E., Ravizza, T., Zurolo, E., Vezzani, A., 2012. Astrocyte immune responses in epilepsy. Glia 60, 1258–1268. https://doi.org/10.1002/glia.22312.

Babcock-Atkinson, E., Norenberg, M.D., Norenberg, L.O.B., Neary, J.T., 1989. Calcium/Calmodulin-dependent protein kinase activity in primary astrocyte cultures. Glia 2, 112–118. https://doi.org/10.1002/glia.440020207.

Bayraktar, O.A., Bartels, T., Holmqvist, S., Kleshchevnikov, V., Martirosyan, A., Polioudakis, D., Ben Haim, L., Young, A.M.H., Batiuk, M.Y., Prakash, K., Brown, A., Roberts, K., Paredes, M.F., Kawaguchi, R., Stockley, J.H., Sabeur, K., Chang, S.M., Huang, E., Hutchinson, P., Ullian, E.M., Hemberg, M., Coppola, G., Holt, M.G., Geschwind, D.H., Rowitch, D.H., 2020. Astrocyte layers in the mammalian cerebral cortex revealed by a single-cell in situ transcriptomic map. Nature Neuroscience 23, 500–509. https://doi.org/10.1038/s41593-020-0602-1.

Beard, E., Lengacher, S., Dias, S., Magistretti, P.J., Finsterwald, C., 2022. Astrocytes as key regulators of brain energy metabolism: new therapeutic perspectives. Frontiers in Physiology 12, 825816. https://doi.org/10.3389/fphys.2021.825816.

Becker, S., Nold, A., Tchumatchenko, T., 2022. Modulation of working memory duration by synaptic and astrocytic mechanisms. PLOS Computational Biology 18, e1010543. https://doi.org/10.1371/journal.pcbi.1010543.

Bellot-Saez, A., Kékesi, O., Morley, J.W., Buskila, Y., 2017. Astrocytic modulation of neuronal excitability through K^+ spatial buffering. Neuroscience and Biobehavioral Reviews 77, 87–97. https://doi.org/10.1016/j.neubiorev.2017.03.002.

Benarroch, E.E., 2016. Astrocyte signaling and synaptic homeostasis: I: Membrane channels, transporters, and receptors in astrocytes. Neurology 87, 324–330. https://doi.org/10.1212/WNL.0000000000002875.

Bergles, D.E., Jahr, C.E., 1997. Synaptic activation of glutamate transporters in hippocampal astrocytes. Neuron 19, 1297–1308. https://doi.org/10.1016/S0896-6273(00)80420-1.

Bergles, D.E., Tzingounis, A.V., Jahr, C.E., 2002. Comparison of coupled and uncoupled currents during glutamate uptake by glt-1 transporters. The Journal of Neuroscience 22, 10153–10162. https://doi.org/10.1523/JNEUROSCI.22-23-10153.2002.

Boison, D., Steinhäuser, C., 2018. Epilepsy and astrocyte energy metabolism. Glia 66, 1235–1243. https://doi.org/10.1002/glia.23247.

Borjkhani, M., Bahrami, F., Janahmadi, M., 2018. Formation of opioid-induced memory and its prevention: a computational study. Frontiers in Computational Neuroscience 12. https://doi.org/10.3389/fncom.2018.00063.

Boucher, J., Kröger, H., Sík, A., 2010. Realistic modelling of receptor activation in hippocampal excitatory synapses: analysis of multivesicular release, release location, temperature and synaptic cross-talk. Brain Structure and Function 215, 49–65. https://doi.org/10.1007/s00429-010-0273-x.

Byrne, J.H., Roberts, J.L., 2004. From Molecules to Networks: An Introduction to Cellular and Molecular Neuroscience. Elsevier Academic Press, Amsterdam.

Campbell, S.L., Hablitz, J.J., Olsen, M.L., 2014. Functional changes in glutamate transporters and astrocyte biophysical properties in a rodent model of focal cortical dysplasia. Frontiers in Cellular Neuroscience 8. https://doi.org/10.3389/fncel.2014.00425.

Carmignoto, G., Gómez-Gonzalo, M., 2010. The contribution of astrocyte signalling to neurovascular coupling. Brain Research Reviews, Synaptic Processes - the role of glial cells 63, 138–148. https://doi.org/10.1016/j.brainresrev.2009.11.007.

Carmignoto, G., Haydon, P.G., 2012. Astrocyte calcium signaling and epilepsy. Glia 60, 1227–1233. https://doi.org/10.1002/glia.22318.

Carnevale, N.T., 2006. The NEURON Book. University Press, Cambridge.

Castel, H., Diallo, M., Chatenet, D., Leprince, J., Desrues, L., Schouft, M.-T., Fontaine, M., Dubessy, C., Lihrmann, I., Scalbert, E., Malagon, M., Vaudry, H., Tonon, M.-C., Gandolfo, P., 2006. Biochemical and functional characterization of high-affinity urotensin II receptors in rat cortical astrocytes. Journal of Neurochemistry 99, 582–595. https://doi.org/10.1111/j.1471-4159.2006.04130.x.

Chai, H., Diaz-Castro, B., Shigetomi, E., Monte, E., Octeau, J.C., Yu, X., Cohn, W., Rajendran, P.S., Vondriska, T.M., Whitelegge, J.P., Coppola, G., Khakh, B.S., 2017. Neural circuit-specialized astrocytes: transcriptomic, proteomic, morphological, and functional evidence. Neuron 95, 531-549.e9. https://doi.org/10.1016/j.neuron.2017.06.029.

Chatton, J.-Y., Magistretti, P.J., Barros, L.F., 2016. Sodium signaling and astrocyte energy metabolism. Glia 64, 1667–1676. https://doi.org/10.1002/glia.22971.

Chistyakov, D.V., Aleshin, S.E., Astakhova, A.A., Sergeeva, M.G., Reiser, G., 2015. Regulation of peroxisome proliferator-activated receptors (PPAR) α and -γ of rat brain astrocytes in the course of activation by toll-like receptor agonists. Journal of Neurochemistry 134, 113–124. https://doi.org/10.1111/jnc.13101.

Choi, H.J., Sun, D., Jakobs, T.C., 2015. Astrocytes in the optic nerve head express putative mechanosensitive channels. Molecular Vision 21, 749–766.

Chowen, J.A., Argente-Arizón, P., Freire-Regatillo, A., Frago, L.M., Horvath, T.L., Argente, J., 2016. The role of astrocytes in the hypothalamic response and adaptation to metabolic signals. Progress in Neurobiology, Targeting Astrocytes in Brain Injuries: A Translational Research Approach 144, 68–87. https://doi.org/10.1016/j.pneurobio.2016.03.001.

Colombo, E., Cordiglieri, C., Melli, G., Newcombe, J., Krumbholz, M., Parada, L.F., Medico, E., Hohlfeld, R., Meinl, E., Farina, C., 2012. Stimulation of the neurotrophin receptor TrkB on astrocytes drives nitric oxide production and neurodegeneration. The Journal of Experimental Medicine 209, 521–535. https://doi.org/10.1084/jem.20110698.

Dal Prà, I., Chiarini, A., Pacchiana, R., Gardenal, E., Chakravarthy, B., Whitfield, J.F., Armato, U., 2014. Calcium-sensing receptors of human astrocyte-neuron teams: amyloid-β-driven mediators and therapeutic targets of Alzheimer's disease. Current Neuropharmacology 12, 353–364. https://doi.org/10.2174/1570159X12666140828214701.

Dave, S., Chen, L., Yu, C., Seaton, M., Khodr, C.E., Al-Harthi, L., Hu, X.-T., 2019. Methamphetamine decreases K^+ channel function in human fetal astrocytes by activating the trace amine-associated receptor type-1. Journal of Neurochemistry 148, 29–45. https://doi.org/10.1111/jnc.14606.

Denizot, A., Arizono, M., Nägerl, U.V., Soula, H., Berry, H., 2019. Simulation of calcium signaling in fine astrocytic processes: Effect of spatial properties on spontaneous activity. PLoS Computational Biology 15, e1006795–e1006795. https://doi.org/10.1371/journal.pcbi.1006795.

Diamond, J.S., 2005. Deriving the glutamate clearance time course from transporter currents in CA1 hippocampal astrocytes: transmitter uptake gets faster during development. The Journal of Neuroscience 25, 2906–2916. https://doi.org/10.1523/JNEUROSCI.5125-04.2005.

Diamond, J.S., Bergles, D.E., Jahr, C.E., 1998. Glutamate release monitored with astrocyte transporter currents during LTP. Neuron 21, 425–433. https://doi.org/10.1016/S0896-6273(00)80551-6.

Du, F., Qian, C., Ming Qian, Z., Wu, X.-M., Xie, H., Yung, W.-H., Ke, Y., 2011. Hepcidin directly inhibits transferrin receptor 1 expression in astrocytes via a cyclic AMP-protein kinase a pathway. Glia 59, 936–945. https://doi.org/10.1002/glia.21166.

Durand, D., Turati, J., Rudi, M.J., Ramírez, D., Saba, J., Caruso, C., Carniglia, L., von Bernhardi, R., Lasaga, M., 2019. Unraveling the β-amyloid clearance by astrocytes: Involvement of metabotropic glutamate receptor 3, sAPPα, and class-A scavenger receptor. Neurochemistry International 131, 104547. https://doi.org/10.1016/j.neuint.2019.104547.

Engels, M., Kalia, M., Rahmati, S., Petersilie, L., Kovermann, P., van Putten, M.J., Rose, C.R., Meijer, H.G., Gensch, T., Fahlke, C., 2021. Glial chloride homeostasis under transient ischemic stress. Frontiers in Cellular Neuroscience 15, 735300–735300. https://doi.org/10.3389/fncel.2021.735300.

Ficker, C., Rozmer, K., Kató, E., Andó, R.D., Schumann, L., Krügel, U., Franke, H., Sperlágh, B., Riedel, T., Illes, P., 2014. Astrocyte-neuron interaction in the substantia gelatinosa of the spinal cord dorsal horn via P2X7 receptor-mediated release of glutamate and reactive oxygen species. Glia 62, 1671–1686. https://doi.org/10.1002/glia.22707.

Flanagan, B., McDaid, L., Wade, J., Wong-Lin, K., Harkin, J., 2018. A computational study of astrocytic glutamate influence on post-synaptic neuronal excitability. PLoS

Computational Biology 14, e1006040–e1006040. https://doi.org/10.1371/journal.pcbi.1006040.

Flanagan, B., McDaid, L., Wade, J.J., Toman, M., Wong-Lin, K., Harkin, J., 2021. A computational study of astrocytic GABA release at the glutamatergic synapse: EAAT-2 and GAT-3 coupled dynamics. Frontiers in Cellular Neuroscience 15, 682460–682460. https://doi.org/10.3389/fncel.2021.682460.

Gao, Y., Layritz, C., Legutko, B., Eichmann, T.O., Laperrousaz, E., Moullé, V.S., Cruciani-Guglielmacci, C., Magnan, C., Luquet, S., Woods, S.C., Eckel, R.H., Yi, C.-X., Garcia-Caceres, C., Tschöp, M.H., 2017. Disruption of lipid uptake in astroglia exacerbates diet-induced obesity. Diabetes (New York, N.Y.) 66, 2555–2563. https://doi.org/10.2337/db16-1278.

Gavrilyuk, V., Kalinin, S., Hilbush, B.S., Middlecamp, A., McGuire, S., Pelligrino, D., Weinberg, G., Feinstein, D.L., 2005. Identification of complement 5a-like receptor (C5L2) from astrocytes: characterization of anti-inflammatory properties. Journal of Neurochemistry 92, 1140–1149. https://doi.org/10.1111/j.1471-4159.2004.02942.x.

Grewer, C., Watzke, N., Wiessner, M., Rauen, T., 2000. Glutamate translocation of the neuronal glutamate transporter EAAC1 occurs within milliseconds. Proceedings of the National Academy of Sciences of the United States of America 97, 9706–9711. https://doi.org/10.1073/pnas.160170397.

Hasel, P., Liddelow, S.A., 2021. Astrocytes. Current Biology 31, R326–R327. https://doi.org/10.1016/j.cub.2021.01.056.

Hay, E., Hill, S., Schürmann, F., Markram, H., Segev, I., 2011. Models of neocortical layer 5b pyramidal cells capturing a wide range of dendritic and perisomatic active properties. PLoS Computational Biology 7, e1002107–e1002107. https://doi.org/10.1371/journal.pcbi.1002107.

Haim, L.B., Rowitch, D.H., 2017. Functional diversity of astrocytes in neural circuit regulation. Nature Reviews Neuroscience 18, 31–41. https://doi.org/10.1038/nrn.2016.159.

Heinemann, U., Kaufer, D., Friedman, A., 2012. Blood-brain barrier dysfunction, TGFβ signaling, and astrocyte dysfunction in epilepsy. Glia 60, 1251–1257. https://doi.org/10.1002/glia.22311.

Héja, L., Szabó, Z., Péter, M., Kardos, J., 2021. Spontaneous Ca^{2+} fluctuations arise in thin astrocytic processes with real 3D geometry. Frontiers in Cellular Neuroscience 15, 617989–617989. https://doi.org/10.3389/fncel.2021.617989.

Hepburn, I., Chen, W., Wils, S., De Schutter, E., 2012. STEPS: efficient simulation of stochastic reaction-diffusion models in realistic morphologies. BMC Systems Biology 6, 36–36. https://doi.org/10.1186/1752-0509-6-36.

Hertz, L., 1979. Functional interactions between neurons and astrocytes I. Turnover and metabolism of putative amino acid transmitters. Progress in Neurobiology 13, 277–323. https://doi.org/10.1016/0301-0082(79)90018-2.

Hong, S.-I., Kang, S., Baker, M., Choi, D.-S., 2021. Astrocyte-neuron interaction in the dorsal striatum-pallidal circuits and alcohol-seeking behaviors. Neuropharmacology 198, 108759–108759. https://doi.org/10.1016/j.neuropharm.2021.108759.

Huang, J., Liu, Y., Cheng, L., Li, J., Zhang, T., Zhao, G., Zhang, H., 2020. Glucagon-like peptide-1 cleavage product GLP-1(9–36) reduces neuroinflammation from stroke via the activation of insulin-like growth factor 1 receptor in astrocytes. European Journal of Pharmacology 887, 173581. https://doi.org/10.1016/j.ejphar.2020.173581.

Huang, X.-J., Zhang, W.-P., Li, C.-T., Shi, W.-Z., Fang, S.-H., Lu, Y.-B., Chen, Z., Wei, E.-Q., 2008. Activation of CysLT receptors induces astrocyte proliferation and death after oxygen–glucose deprivation. Glia 56, 27–37. https://doi.org/10.1002/glia.20588.

Hübel, N., Hosseini-Zare, M.S., Žiburkus, J., Ullah, G., 2017. The role of glutamate in neuronal ion homeostasis: A case study of spreading depolarization. PLoS Computational Biology 13, e1005804–e1005804. https://doi.org/10.1371/journal.pcbi.1005804.

Ibáñez, I., Bartolomé-Martín, D., Piniella, D., Giménez, C., Zafra, F., 2019. Activity dependent internalization of the glutamate transporter GLT-1 requires calcium entry through the NCX sodium/calcium exchanger. Neurochemistry International 123, 125–132. https://doi.org/10.1016/j.neuint.2018.03.012.

Ibrahim, M.M.H., Alhamami, H.N., Briski, K.P., 2019. Norepinephrine regulation of ventromedial hypothalamic nucleus metabolic transmitter biomarker and astrocyte enzyme and receptor expression: Impact of 5′ AMP-activated protein kinase. Brain Research 1711, 48–57. https://doi.org/10.1016/j.brainres.2019.01.012.

Inazu, M., Takeda, H., Matsumiya, T., 2005. Molecular and functional characterization of an Na+-independent choline transporter in rat astrocytes. Journal of Neurochemistry 94, 1427–1437. https://doi.org/10.1111/j.1471-4159.2005.03299.x.

Ingiosi, A.M., Opp, M.R., 2016. Sleep and immunomodulatory responses to systemic lipopolysaccharide in mice selectively expressing interleukin-1 receptor 1 on neurons or astrocytes. Glia 64, 780–791. https://doi.org/10.1002/glia.22961.

Iovino, L., Giusti, V., Pischedda, F., Giusto, E., Plotegher, N., Marte, A., Battisti, I., Di Iacovo, A., Marku, A., Piccoli, G., Bandopadhyay, R., Perego, C., Bonifacino, T., Bonanno, G., Roseti, C., Bossi, E., Arrigoni, G., Bubacco, L., Greggio, E., Hilfiker, S., Civiero, L., 2022. Trafficking of the glutamate transporter is impaired in LRRK2-related Parkinson's disease. Acta Neuropathologica 144, 81–106. https://doi.org/10.1007/s00401-022-02437-0.

Iseki, K., Hagino, S., Mori, T., Zhang, Y., Yokoya, S., Takaki, H., Tase, C., Murakawa, M., Wanaka, A., 2002. Increased syndecan expression by pleiotrophin and FGF receptor-expressing astrocytes in injured brain tissue. Glia 39, 1–9. https://doi.org/10.1002/glia.10078.

Ivens, S., Kaufer, D., Flores, L.P., Bechmann, I., Zumsteg, D., Tomkins, O., Seiffert, E., Heinemann, U., Friedman, A., 2007. TGF-β receptor-mediated albumin uptake into astrocytes is involved in neocortical epileptogenesis. Brain 130, 535–547. https://doi.org/10.1093/brain/awl317.

Jackson, J.G., O'Donnell, J.C., Takano, H., Coulter, D.A., Robinson, M.B., 2014. Neuronal activity and glutamate uptake decrease mitochondrial mobility in astrocytes and position mitochondria near glutamate transporters. The Journal of Neuroscience 34, 1613–1624. https://doi.org/10.1523/JNEUROSCI.3510-13.2014.

Jaudon, F., Chiacchiaretta, M., Albini, M., Ferroni, S., Benfenati, F., Cesca, F., 2020. Kidins220/ARMS controls astrocyte calcium signaling and neuron-astrocyte communication. Cell Death and Differentiation 27, 1505–1519. https://doi.org/10.1038/s41418-019-0431-5.

Jayakumar, A.R., Valdes, V., Tong, X.Y., Shamaladevi, N., Gonzalez, W., Norenberg, M.D., 2014. Sulfonylurea receptor 1 contributes to the astrocyte swelling and brain edema in acute liver failure. Translational Stroke Research 5, 28–37. https://doi.org/10.1007/s12975-014-0328-z.

Johnson, E.C.B., Dammer, E.B., Duong, D.M., Ping, L., Zhou, M., Yin, L., Higginbotham, L.A., Guajardo, A., White, B., Troncoso, J.C., Thambisetty, M., Montine, T.J., Lee, E.B., Trojanowski, J.Q., Beach, T.G., Reiman, E.M., Haroutunian, V., Wang, M., Schadt, E., Zhang, B., Dickson, D.W., Ertekin-Taner, N., Golde, T.E., Petyuk, V.A., De Jager, P.L., Bennett, D.A., Wingo, T.S., Rangaraju, S., Hajjar, I., Shulman, J.M., Lah, J.J., Levey, A.I., Seyfried, N.T., 2020. Large-scale proteomic analysis of Alzheimer's disease brain and cerebrospinal fluid reveals early changes in energy metabolism associated with microglia and astrocyte activation. Nature Medicine 26, 769–780. https://doi.org/10.1038/s41591-020-0815-6.

Jolivet, R., Coggan, J.S., Allaman, I., Magistretti, P.J., 2015. Multi-timescale modeling of activity-dependent metabolic coupling in the neuron-glia-vasculature ensemble. PLoS Computational Biology 11, e1004036–e1004036. https://doi.org/10.1371/journal.pcbi.1004036.

Jolly, S., Bazargani, N., Quiroga, A.C., Pringle, N.P., Attwell, D., Richardson, W.D., Li, H., 2018. G protein-coupled receptor 37-like 1 modulates astrocyte glutamate transporters and neuronal NMDA receptors and is neuroprotective in ischemia. Glia 66, 47–61. https://doi.org/10.1002/glia.23198.

Juraszek, B., Nałęcz, K.A., 2016. Protein phosphatase PP2A – a novel interacting partner of carnitine transporter OCTN2 (SLC22A5) in rat astrocytes. Journal of Neurochemistry 139, 537–551. https://doi.org/10.1111/jnc.13777.

Kalia, M., Meijer, H.G.E., van Gils, S.A., van Putten, M.J., Rose, C.R., 2021. Ion dynamics at the energy-deprived tripartite synapse. PLoS Computational Biology 17, e1009019–e1009019. https://doi.org/10.1371/journal.pcbi.1009019.

Kettenmann, H., 2013. Neuroglia, Third edition. ed. Oxford University Press, New York.

Kim, K.J., Iddings, J.A., Stern, J.E., Blanco, V.M., Croom, D., Kirov, S.A., Filosa, J.A., 2015. Astrocyte Contributions to Flow/Pressure-Evoked Parenchymal Arteriole Vasoconstriction. The Journal of Neuroscience 35, 8245–8257. https://doi.org/10.1523/JNEUROSCI.4486-14.2015.

Kirischuk, S., Kettenmann, H., Verkhratsky, A., 2007. Membrane currents and cytoplasmic sodium transients generated by glutamate transport in Bergmann glial cells. Pflügers Archiv - European Journal of Physiology 454, 245–52. https://doi.org/10.1007/s00424-007-0207-5.

Kisler, K., Nelson, A.R., Montagne, A., Zlokovic, B.V., 2017. Cerebral blood flow regulation and neurovascular dysfunction in Alzheimer disease. Nature Reviews Neuroscience 18, 419–434. https://doi.org/10.1038/nrn.2017.48.

Koch, C., 1999. Biophysics of Computation: Information Processing in Single Neurons, Computational neuroscience. Oxford University Press, New York.

Koyama, Y., Hayashi, M., Nagae, R., Tokuyama, S., Konishi, T., 2014. Endothelin-1 increases the expression of VEGF-R1/Flt-1 receptors in rat cultured astrocytes through ETB receptors. Journal of Neurochemistry 130, 759–769. https://doi.org/10.1111/jnc.12770.

Kyriatzis, G., Bernard, A., Bôle, A., Pflieger, G., Chalas, P., Masse, M., Lécorché, P., Jacquot, G., Ferhat, L., Khrestchatisky, M., 2021. Neurotensin receptor 2 is induced in astrocytes and brain endothelial cells in relation to neuroinflammation following pilocarpine-induced seizures in rats. Glia 69, 2618–2643. https://doi.org/10.1002/glia.24062.

Leiss, L., Mega, A., Olsson Bontell, T., Nistér, M., Smits, A., Corvigno, S., Rahman, M.A., Enger, P.Ø., Miletic, H., Östman, A., 2020. Platelet-derived growth factor receptor α/glial fibrillary acidic protein expressing peritumoral astrocytes associate with shorter median overall survival in glioblastoma patients. Glia 68, 979–988. https://doi.org/10.1002/glia.23756.

Li, B., Zhang, S., Zhang, H., Nu, W., Cai, L., Hertz, L., Peng, L., 2008. Fluoxetine-mediated 5-HT2B receptor stimulation in astrocytes causes EGF receptor transactivation and ERK phosphorylation. Psychopharmacologia 201, 443–458. https://doi.org/10.1007/s00213-008-1306-5.

Lisjak, M., Potokar, M., Rituper, B., Jorgačevski, J., Zorec, R., 2017. AQP4e-based orthogonal arrays regulate rapid cell volume changes in astrocytes. The Journal of Neuroscience 37, 10748–10756. https://doi.org/10.1523/JNEUROSCI.0776-17.2017.

Liu, C., Cui, G., Zhu, M., Kang, X., Guo, H., 2014. Neuroinflammation in Alzheimer's disease: chemokines produced by astrocytes and chemokine receptors. International Journal of Clinical and Experimental Pathology 7, 8342–8355.

Lu, L., Hogan-Cann, A.D., Globa, A.K., Lu, P., Nagy, J.I., Bamji, S.X., Anderson, C.M., 2019. Astrocytes drive cortical vasodilatory signaling by activating endothelial NMDA receptors. Journal of Cerebral Blood Flow & Metabolism 39, 481–496. https://doi.org/10.1177/0271678X17734100.

Ma, K., Ding, X., Song, Q., Han, Z., Yao, H., Ding, J., Hu, G., 2020. Lactate enhances Arc/arg3.1 expression through hydroxycarboxylic acid receptor 1-β-arrestin2 pathway in astrocytes. Neuropharmacology 171, 108084. https://doi.org/10.1016/j.neuropharm.2020.108084.

Malynn, S., Campos-Torres, A., Moynagh, P., Haase, J., 2013. The pro-inflammatory cytokine TNF-α regulates the activity and expression of the serotonin transporter (SERT) in astrocytes. Neurochemical Research 38, 694–704. https://doi.org/10.1007/s11064-012-0967-y.

Manaserh, I.H., Chikkamenahalli, L., Ravi, S., Dube, P.R., Park, J.J., Hill, J.W., 2019. Ablating astrocyte insulin receptors leads to delayed puberty and hypogonadism in mice. PLoS Biology 17, e3000189. https://doi.org/10.1371/journal.pbio.3000189.

Manninen, T., Aćimović, J., Linne, M.-L., 2023. Analysis of network models with neuron-astrocyte interactions. Neuroinformatics 21, 375–406. https://doi.org/10.1007/s12021-023-09622-w.

Manninen, T., Havela, R., Linne, M.-L., 2018. Computational models for calcium-mediated astrocyte functions. Frontiers in Computational Neuroscience 12, 14–14. https://doi.org/10.3389/fncom.2018.00014.

Manninen, T., Saudargiene, A., Linne, M.-L., 2020. Astrocyte-mediated spike-timing-dependent long-term depression modulates synaptic properties in the developing cortex. PLoS Computational Biology 16, e1008360–e1008360. https://doi.org/10.1371/journal.pcbi.1008360.

Marina, N., Christie, I.N., Korsak, A., Doronin, M., Brazhe, A., Hosford, P.S., Wells, J.A., Sheikhbahaei, S., Humoud, I., Paton, J.F.R., Lythgoe, M.F., Semyanov, A., Kasparov, S., Gourine, A.V., 2020. Astrocytes monitor cerebral perfusion and control systemic circulation to maintain brain blood flow. Nature Communications 11, 131. https://doi.org/10.1038/s41467-019-13956-y.

Matos, M., Augusto, E., Agostinho, P., Cunha, R.A., Chen, J.-F., 2013. Antagonistic interaction between adenosine A2A receptors and Na^+/K^+-ATPase-α2 controlling glutamate uptake in astrocytes. The Journal of Neuroscience 33, 18492–18502. https://doi.org/10.1523/JNEUROSCI.1828-13.2013.

Mazaud, D., Capano, A., Rouach, N., 2021. The many ways astroglial connexins regulate neurotransmission and behavior. Glia 69, 2527–2545. https://doi.org/10.1002/glia.24040.

McDougal, R.A., Morse, T.M., Carnevale, T., Marenco, L., Wang, R., Migliore, M., Miller, P.L., Shepherd, G.M., Hines, M.L., 2017. Twenty years of ModelDB and beyond: building essential modeling tools for the future of neuroscience. Journal of Computational Neuroscience 42, 1–10. https://doi.org/10.1007/s10827-016-0623-7.

Mele, T., Jurič, D.M., 2013. Identification and pharmacological characterization of the histamine H3 receptor in cultured rat astrocytes. European Journal of Pharmacology 720, 198–204. https://doi.org/10.1016/j.ejphar.2013.10.028.

Min, R., Nevian, T., 2012. Astrocyte signaling controls spike timing-dependent depression at neocortical synapses. Nature Neuroscience 15, 746–53. https://doi.org/10.1038/nn.3075.

Min, R., van der Knaap, M.S., 2018. Genetic defects disrupting glial ion and water homeostasis in the brain. Brain Pathology 28, 372–387. https://doi.org/10.1111/bpa.12602.

Miquel, J., Haymaker, W., 1965. Astroglial reactions to ionizing radiation: with emphasis on glycogen accumulation, in: Biology of Neuroglia. Elsevier Science & Technology, The Netherlands, pp. 89–114. https://doi.org/10.1016/S0079-6123(08)60941-3.

Mizuno, G.O., Wang, Yinxue, Shi, G., Wang, Yizhi, Sun, J., Papadopoulos, S., Broussard, G.J., Unger, E.K., Deng, W., Weick, J., Bhattacharyya, A., Chen, C.-Y., Yu, G., Looger, L.L., Tian, L., 2018. Aberrant calcium signaling in astrocytes inhibits neuronal excitability in a human down syndrome stem cell model. Cell Reports (Cambridge) 24, 355–365. https://doi.org/10.1016/j.celrep.2018.06.033.

Montoya, A., Elgueta, D., Campos, J., Chovar, O., Falcón, P., Matus, S., Alfaro, I., Bono, M.R., Pacheco, R., 2019. Dopamine receptor D3 signalling in astrocytes promotes neuroinflammation. Journal of Neuroinflammation 16, 258. https://doi.org/10.1186/s12974-019-1652-8.

Müller, F.E., Schade, S.K., Cherkas, V., Stopper, L., Breithausen, B., Minge, D., Varbanov, H., Wahl-Schott, C., Antoniuk, S., Domingos, C., Compan, V., Kirchhoff, F., Henneberger, C., Ponimaskin, E., Zeug, A., 2021. Serotonin receptor 4 regulates hippocampal astrocyte morphology and function. Glia 69, 872–889. https://doi.org/10.1002/glia.23933.

Mullershausen, F., Craveiro, L.M., Shin, Y., Cortes-Cros, M., Bassilana, F., Osinde, M., Wishart, W.L., Guerini, D., Thallmair, M., Schwab, M.E., Sivasankaran, R., Seuwen, K., Dev, K.K., 2007. Phosphorylated FTY720 promotes astrocyte migration through sphingosine-1-phosphate receptors. Journal of Neurochemistry 102, 1151–1161. https://doi.org/10.1111/j.1471-4159.2007.04629.x.

Murai, K.K., Pasquale, E.B., 2011. Eph receptors and ephrins in neuron-astrocyte communication at synapses. Glia 59, 1567–1578. https://doi.org/10.1002/glia.21226.

Nam, M.-H., Han, K.-S., Lee, J., Bae, J.Y., An, H., Park, S., Oh, S.-J., Kim, E., Hwang, E., Bae, Y.C., Lee, C.J., 2018. Expression of μ-opioid receptor in CA1 hippocampal astrocytes. Experimental Neurobiology 27, 120–128. https://doi.org/10.5607/en.2018.27.2.120.

Naranjo, V., Contreras, A., Merino, B., Plaza, A., Lorenzo, M.P., García-Cáceres, C., García, A., Chowen, J.A., Ruiz-Gayo, M., Del Olmo, N., Cano, V., 2020. Specific deletion of the astrocyte leptin receptor induces changes in hippocampus glutamate metabolism, synaptic transmission and plasticity. Neuroscience, The Neuroscience of Energy Balance and Eating Behavior 447, 182–190. https://doi.org/10.1016/j.neuroscience.2019.10.005.

NEURON (2020) The Neuron Forum. Available at: www.neuron.yale.edu/phpBB (Accessed: 8 May 2023).

Nippert, A.R., Chiang, P.-P., Del Franco, A.P., Newman, E.A., 2022. Astrocyte regulation of cerebral blood flow during hypoglycemia. Journal of Cerebral Blood Flow & Metabolism 42, 1534–1546. https://doi.org/10.1177/0271678X221089091.

Nortley, R., Attwell, D., 2017. Control of brain energy supply by astrocytes. Current Opinion in Neurobiology 47, 80–85. https://doi.org/10.1016/j.conb.2017.09.012.

O'Connor, A.T., Clark, M.A., Trivedi, M., 2018. Interaction between the dopamine D4 receptor and the angiotensin II type 1 receptor in rat astrocytes. The FASEB Journal 32, lb611–lb611. https://doi.org/10.1096/fasebj.2018.32.1_supplement.lb611.

Okubo, Y., 2020. Astrocytic Ca2+ signaling mediated by the endoplasmic reticulum in health and disease. Journal of Pharmacological Sciences 144, 83–88. https://doi.org/10.1016/j.jphs.2020.07.006.

Olsen, M.L., Khakh, B.S., Skatchkov, S.N., Zhou, M., Lee, C.J., Rouach, N., 2015. New insights on astrocyte ion channels: critical for homeostasis and neuron-glia signaling. The Journal of Neuroscience 35, 13827–13835. https://doi.org/10.1523/JNEUROSCI.2603-15.2015.

Olson, J.E., Evers, J.A., 1992. Correlations between energy metabolism, ion transport, and water content in astrocytes. Canadian Journal of Physiology and Pharmacology 70, S350–S355. https://doi.org/10.1139/y92-282.

Onodera, M., Meyer, J., Furukawa, K., Hiraoka, Y., Aida, T., Tanaka, K., Tanaka, K.F., Rose, C.R., Matsui, K., 2021. Exacerbation of epilepsy by astrocyte alkalization and gap junction uncoupling. The Journal of Neuroscience 41, 2106–2118. https://doi.org/10.1523/JNEUROSCI.2365-20.2020.

Oschmann, F., Mergenthaler, K., Jungnickel, E., Obermayer, K., 2017. Spatial separation of two different pathways accounting for the generation of calcium signals in astrocytes. PLoS Computational Biology 13, e1005377. https://doi.org/10.1371/journal.pcbi.1005377.

Paniagua-Herranz, L., Gil-Redondo, J.C., Queipo, M.J., González-Ramos, S., Boscá, L., Pérez-Sen, R., Miras-Portugal, M.T., Delicado, E.G., 2017. Prostaglandin E2 impairs P2Y2/P2Y4 receptor signaling in cerebellar astrocytes via EP3 receptors. Frontiers in Pharmacology 8. https://doi.org/10.3389/fphar.2017.00937.

Parpura, V., Haydon, P.G., 2009. Astrocytes in (Patho)Physiology of the Nervous System, 1. Aufl. ed. Springer-Verlag, New York, NY.

Paulson, O.B., Newman, E.A., 1987. Does the release of potassium from astrocyte endfeet regulate cerebral blood flow? Science (American Association for the Advancement of Science) 237, 896–898. https://doi.org/10.1126/science.3616619.

Peterson, A.R., Garcia, T.A., Cullion, K., Tiwari-Woodruff, S.K., Pedapati, E.V., Binder, D.K., 2021. Targeted overexpression of glutamate transporter-1 reduces seizures and attenuates pathological changes in a mouse model of epilepsy. Neurobiology of Disease 157, 105443–105443. https://doi.org/10.1016/j.nbd.2021.105443.

Petr, G.T., Sun, Y., Frederick, N.M., Zhou, Y., Dhamne, S.C., Hameed, M.Q., Miranda, C., Bedoya, E.A., Fischer, K.D., Armsen, W., Wang, J., Danbolt, N.C., Rotenberg, A., Aoki, C.J., Rosenberg, P.A., 2015. Conditional deletion of the glutamate transporter glt-1 reveals that astrocytic GLT-1 protects against fatal epilepsy while neuronal GLT-1 contributes significantly to glutamate uptake into synaptosomes. The Journal of Neuroscience 35, 5187–5201. https://doi.org/10.1523/JNEUROSCI.4255-14.2015.

Podda, M.V., Leone, L., Piacentini, R., Cocco, S., Mezzogori, D., D'Ascenzo, M., Grassi, C., 2012. Expression of olfactory-type cyclic nucleotide-gated channels in rat cortical astrocytes. Glia 60, 1391–1405. https://doi.org/10.1002/glia.22360.

Pollen, D.A., 1973. Focal epilepsy and the neuroglial impairment hypothesis, in: UCLA Forum in Medical Sciences. pp. 29–35. https://doi.org/10.1016/B978-0-12-128650-7.50008-1.

Prevot, V., Rio, C., Cho, G.J., Lomniczi, A., Heger, S., Neville, C.M., Rosenthal, N.A., Ojeda, S.R., Corfas, G., 2003. Normal female sexual development requires neuregulin–erbb receptor signaling in hypothalamic astrocytes. The Journal of Neuroscience 23, 230–239. https://doi.org/10.1523/JNEUROSCI.23-01-00230.2003.

Purnell, B.S., Alves, M., Boison, D., 2023. Astrocyte-neuron circuits in epilepsy. Neurobiology of disease 179, 106058–106058. https://doi.org/10.1016/j.nbd.2023.106058.

Quintana, A., Erta, M., Ferrer, B., Comes, G., Giralt, M., Hidalgo, J., 2013. Astrocyte-specific deficiency of interleukin-6 and its receptor reveal specific roles in survival, body weight and behavior. Brain, Behavior, and Immunity 27, 162–173. https://doi.org/10.1016/j.bbi.2012.10.011.

Reiner, D.J., Mietlicki-Baase, E.G., McGrath, L.E., Zimmer, D.J., Bence, K.K., Sousa, G.L., Konanur, V.R., Krawczyk, J., Burk, D.H., Kanoski, S.E., Hermann, G.E., Rogers, R.C., Hayes, M.R., 2016. Astrocytes regulate GLP-1 receptor-mediated effects on energy balance. The Journal of Neuroscience 36, 3531–3540. https://doi.org/10.1523/JNEUROSCI.3579-15.2016.

Reynolds, J.A., Johnson, E.A., Tanford, C., 1985. Incorporation of membrane potential into theoretical analysis of electrogenic ion pumps. Proceedings of the National Academy of Sciences - PNAS 82, 6869–6873. https://doi.org/10.1073/pnas.82.20.6869.

Rimmele, T.S., Rocher, A.-B., Wellbourne-Wood, J., Chatton, J.-Y., 2017. Control of glutamate transport by extracellular potassium: basis for a negative feedback on synaptic transmission. Cerebral Cortex (New York, N.Y. 1991) 27, 3272–3283. https://doi.org/10.1093/cercor/bhx078.

Rojas, H., Colina, C., Ramos, M., Benaim, G., Jaffe, E.H., Caputo, C., DiPolo, R., 2007. Na^+ entry via glutamate transporter activates the reverse Na^+/Ca^{2+} exchange and triggers -induced Ca^{2+} release in rat cerebellar Type-1 astrocytes. Journal of Neurochemistry 100, 1188–1202. https://doi.org/10.1111/j.1471-4159.2006.04303.x.

Rosciszewski, G., Cadena, V., Murta, V., Lukin, J., Villarreal, A., Roger, T., Ramos, A.J., 2018. Toll-like receptor 4 (TLR4) and triggering receptor expressed on myeloid cells-2 (TREM-2) activation balance astrocyte polarization into a proinflammatory phenotype. Molecular Neurobiology 55, 3875–3888. https://doi.org/10.1007/s12035-017-0618-z.

Rose, C.R., Karus, C., 2013. Two sides of the same coin: Sodium homeostasis and signaling in astrocytes under physiological and pathophysiological conditions. Glia 61, 1191–1205. https://doi.org/10.1002/glia.22492.

Rosenegger, D.G., Tran, C.H.T., Wamsteeker Cusulin, J.I., Gordon, G.R., 2015. Tonic local brain blood flow control by astrocytes independent of phasic neurovascular coupling. The Journal of Neuroscience 35, 13463–13474. https://doi.org/10.1523/JNEUROSCI.1780-15.2015.

Rusakov, D.A., 2015. Disentangling calcium-driven astrocyte physiology. Nature reviews. Neuroscience 16, 226–233. https://doi.org/10.1038/nrn3878.

Rusakov, D.A., Kullmann, D.M., 1998. Extrasynaptic glutamate diffusion in the hippocampus: ultrastructural constraints, uptake, and receptor activation. The Journal of Neuroscience 18, 3158–3170. https://doi.org/10.1523/JNEUROSCI.18-09-03158.1998.

Samluk, Ł., Czeredys, M., Nałęcz, K.A., 2010. Regulation of amino acid/carnitine transporter B0,+ (ATB0,+) in astrocytes by protein kinase C: independent effects on raft and non-raft transporter subpopulations. Journal of Neurochemistry 115, 1386–1397. https://doi.org/10.1111/j.1471-4159.2010.07040.x.

Sato, K., Malchinkhuu, E., Horiuchi, Y., Mogi, C., Tomura, H., Tosaka, M., Yoshimoto, Y., Kuwabara, A., Okajima, F., 2007. Critical role of ABCA1 transporter in sphingosine 1-phosphate release from astrocytes. Journal of Neurochemistry 103, 2610–2619. https://doi.org/10.1111/j.1471-4159.2007.04958.x.

Sato, K., Matsuki, N., Ohno, Y., Nakazawa, K., 2003. Estrogens inhibit l-glutamate uptake activity of astrocytes via membrane estrogen receptor α. Journal of Neurochemistry 86, 1498–1505. https://doi.org/10.1046/j.1471-4159.2003.01953.x.

Savtchenko, L.P., Bard, L., Jensen, T.P., Reynolds, J.P., Kraev, I., Medvedev, N., Stewart, M.G., Henneberger, C., Rusakov, D.A., 2018. Disentangling astroglial physiology with a realistic cell model in silico. Nature Communications 9, 3554–15. https://doi.org/10.1038/s41467-018-05896-w.

Schipper, H.M., 1991. Gomori-positive astrocytes: Biological properties and implications for neurologic and neuroendocrine disorders. Glia 4, 365–377. https://doi.org/10.1002/glia.440040404.

Schousboe, A., Svenneby, G., Hertz, L., 1977. Uptake and metabolism of glutamate in astrocytes cultured from dissociated mouse brain hemispheres. Journal of Neurochemistry 29, 999–1005. https://doi.org/10.1111/j.1471-4159.1977.tb06503.x.

Semyanov, A., Henneberger, C., Agarwal, A., 2020. Making sense of astrocytic calcium signals — from acquisition to interpretation. Nature Reviews Neuroscience 21, 551–564. https://doi.org/10.1038/s41583-020-0361-8.

Seppälä, Ylihärsilä, Manninen, Linne, manuscript in preparation.

Silverman, W.R., de Rivero Vaccari, J.P., Locovei, S., Qiu, F., Carlsson, S.K., Scemes, E., Keane, R.W., Dahl, G., 2009. The pannexin 1 channel activates the inflammasome in neurons and astrocytes. The Journal of Biological Chemistry 284, 18143–18151. https://doi.org/10.1074/jbc.M109.004804.

Sipe, G.O., Petravicz, J., Rikhye, R.V., Garcia, R., Mellios, N., Sur, M., 2021. Astrocyte glutamate uptake coordinates experience-dependent, eye-specific refinement in developing visual cortex. Glia 69, 1723–1735. https://doi.org/10.1002/glia.23987.

Smith, A.M., Davey, K., Tsartsalis, S., Khozoie, C., Fancy, N., Tang, S.S., Liaptsi, E., Weinert, M., McGarry, A., Muirhead, R.C.J., Gentleman, S., Owen, D.R., Matthews,

P.M., 2022. Diverse human astrocyte and microglial transcriptional responses to Alzheimer's pathology. Acta Neuropathologica 143, 75–91. https://doi.org/10.1007/s00401-021-02372-6.

Smith, C., Toohey, N., Knight, J.A., Klein, M.T., Teitler, M., 2011. Risperidone-induced inactivation and clozapine-induced reactivation of rat cortical astrocyte 5-hydroxytryptamine7 receptors: evidence for in situ G protein-coupled receptor homodimer protomer cross-talk. Molecular Pharmacology 79, 318–325. https://doi.org/10.1124/mol.110.069278.

Sorensen, S.D., Nicole, O., Peavy, R.D., Montoya, L.M., Lee, C.J., Murphy, T.J., Traynelis, S.F., Hepler, J.R., 2003. Common signaling pathways link activation of murine PAR-1, LPA, and S1P receptors to proliferation of astrocytes. Molecular Pharmacology 64, 1199–1209. https://doi.org/10.1124/mol.64.5.1199.

Steinhäuser, C., Seifert, G., Bedner, P., 2012. Astrocyte dysfunction in temporal lobe epilepsy: K+ channels and gap junction coupling. Glia 60, 1192–1202. https://doi.org/10.1002/glia.22313.

Stella, N., 2010. Cannabinoid and cannabinoid-like receptors in microglia, astrocytes, and astrocytomas. Glia 58, 1017–1030. https://doi.org/10.1002/glia.20983.

Sterratt, D., Graham, B., Gillies, A., Willshaw, D., 2011. Principles of Computational Modelling in Neuroscience. University Press, Cambridge. https://doi.org/10.1017/CBO9780511975899.

Takahashi, K., Foster, J.B., Lin, C.G., 2015. Glutamate transporter EAAT2: regulation, function, and potential as a therapeutic target for neurological and psychiatric disease. Cellular and Molecular Life Sciences 72, 3489–3506. https://doi.org/10.1007/s00018-015-1937-8.

Tyurikova, O., Shih, P.-Y., Dembitskaya, Y., Savtchenko, L.P., McHugh, T.J., Rusakov, D.A., Semyanov, A., 2022. K+ efflux through postsynaptic NMDA receptors suppresses local astrocytic glutamate uptake. Glia 70, 961–974. https://doi.org/10.1002/glia.24150.

Umpierre, A.D., West, P.J., White, J.A., Wilcox, K.S., 2019. Conditional knock-out of mGluR5 from astrocytes during epilepsy development impairs high-frequency glutamate uptake. The Journal of Neuroscience 39, 727–742. https://doi.org/10.1523/JNEUROSCI.1148-18.2018.

Unichenko, P., Myakhar, O., Kirischuk, S., 2012. Intracellular Na^+ concentration influences short-term plasticity of glutamate transporter-mediated currents in neocortical astrocytes. Glia 60, 605–614. https://doi.org/10.1002/glia.22294.

Untiet, V., Kovermann, P., Gerkau, N.J., Gensch, T., Rose, C.R., Fahlke, C., 2017. Glutamate transporter-associated anion channels adjust intracellular chloride concentrations during glial maturation. Glia 65, 388–400. https://doi.org/10.1002/glia.23098.

Vandenberg, R.J., Ryan, R.M., 2013. Mechanisms of glutamate transport. Physiological Reviews 93, 1621–1657. https://doi.org/10.1152/physrev.00007.2013.

Verkhratsky, A., Nedergaard, M., 2018. Physiology of Astroglia. Physiological Reviews 98, 239–389. https://doi.org/10.1152/physrev.00042.2016.

Wang, S., Wang, B., Shang, D., Zhang, K., Yan, X., Zhang, X., 2022. Ion channel dysfunction in astrocytes in neurodegenerative diseases. Frontiers in Physiology 13. https://doi.org/10.3389/fphys.2022.814285.

Wang, Y., Luo, W., Reiser, G., 2007. Activation of protease-activated receptors in astrocytes evokes a novel neuroprotective pathway through release of chemokines of the growth-regulated oncogene/cytokine-induced neutrophil chemoattractant family. European Journal of Neuroscience 26, 3159–3168. https://doi.org/10.1111/j.1460-9568.2007.05938.x.

Wang, Y., Zhou, C.-F., 2005. Involvement of interferon-γ and its receptor in the activation of astrocytes in the mouse hippocampus following entorhinal deafferentation. Glia 50, 56–65. https://doi.org/10.1002/glia.20152.

Wanke, E., Gullo, F., Dossi, E., Valenza, G., Becchetti, A., 2016. Neuron-glia cross talk revealed in reverberating networks by simultaneous extracellular recording of spikes and astrocytes' glutamate transporter and K+ currents. Journal of Neurophysiology, Glial Cells and Neuronal Signaling 116, 2706–2719. https://doi.org/10.1152/jn.00509.2016.

Yu, X., Taylor, A.M.W., Nagai, J., Golshani, P., Evans, C.J., Coppola, G., Khakh, B.S., 2018. Reducing astrocyte calcium signaling in vivo alters striatal microcircuits and causes repetitive behavior. Neuron 99, 1170-1187.e9. https://doi.org/10.1016/j.neuron.2018.08.015.

Zhang, H., Xin, W., Dougherty, P.M., 2009. Synaptically evoked glutamate transporter currents in spinal dorsal horn astrocytes. Molecular Pain 5, 1744-8069-5–36. https://doi.org/10.1186/1744-8069-5-36.

Zhang, Z., Chen, H., Geng, Z., Yu, Z., Li, H., Dong, Y., Zhang, H., Huang, Z., Jiang, J., Zhao, Y., 2022. Structural basis of ligand binding modes of human EAAT2. Nature Communications 13, 3329–3329. https://doi.org/10.1038/s41467-022-31031-x.

Zhang, Z., Tao, Z., Gameiro, A., Barcelona, S., Braams, S., Rauen, T., Grewer, C., 2007. Transport direction determines the kinetics of substrate transport by the glutamate transporter EAAC1. Proceedings of the National Academy of Sciences 104, 18025–18030. https://doi.org/10.1073/pnas.0704570104.

Zhao, B., Gu, L., Liu, K., Zhang, M., Liu, H., 2017. Maxi-anion channels play a key role in glutamate-induced ATP release from mouse astrocytes in primary culture. Neuroreport 28, 380–385. https://doi.org/10.1097/WNR.0000000000000759.

Zuidema, J.M., Hyzinski-García, M.C., Van Vlasselaer, K., Zaccor, N.W., Plopper, G.E., Mongin, A.A., Gilbert, R.J., 2014. Enhanced GLT-1 mediated glutamate uptake and migration of primary astrocytes directed by fibronectin-coated electrospun poly-l-lactic acid fibers. Biomaterials 35, 1439–1449. https://doi.org/10.1016/j.biomaterials.2013.10.079.

Zylbertal, A., Yarom, Y., Wagner, S., 2017. The Slow Dynamics of Intracellular Sodium Concentration Increase the Time Window of Neuronal Integration: A Simulation Study. Frontiers in Computational Neuroscience 11, 85–85. https://doi.org/10.3389/fncom.2017.00085.

APPENDIX: GLUTAMATE TRANSPORTER CODE FOR NEURON SIMULATOR

```
NEURON {
   SUFFIX GluT
   RANGE iglu_trans, ina_trans, ik_trans, itotal_trans
   RANGE nain, naout, kin, kout, gluin, gluout
   RANGE total_current
   USEION na READ ina WRITE nai, ina, nao
   USEION k READ ik WRITE ki, ik, ko
   USEION glu READ iglu WRITE glui, iglu, gluo VALENCE -1
}

UNITS {
   (l) = (liter)
   (mV) = (millivolt)
   (mA) = (milliamp)
   (mol) = (1)
   (mmol) = (millimol)
   (mM) = (mmol/l)
   F = (faraday) (kilocoulombs)
   PI = (pi) (1)
   (um) = (micron)
   (uA) = (microamp)
   R = (k-mole) (joule/degC)
}

PARAMETER {
   : Rates
   nasrcrate = 0 (/ms)
   ksrcrate = 0 (/ms)
   glusrcrate = 0 (/ms)

   k12 = 20 (l/mmol-ms)
   k21 = 0.1 (/ms)
   k23 = 0.015 (l/mmol-ms)
   k32 = 0.5 (/ms)
   k34 = 0.2 (/ms)
   k43 = 0.6 (/ms)
   k45 = 4 (/ms)
   k54 = 10 (l/mmol-ms)
   k56 = 1 (/ms)
   k65 = 0.1 (l/mmol-ms)
   k16 = 0.0016 (l/mmol-ms)
   k61 = 2e-4 (l/mmol-ms)

   TotalTrans = 1.66e-12 (mol/cm2)

   nain = 15 (mmol/l)
   naout = 150 (mmol/l)
   kin = 120 (mmol/l)
   kout = 3 (mmol/l)
```

```
50      gluin = 0.3 (mmol/l)
        gluout = 20e-6 (mmol/l)
52
        iter = 1
54  }

56  ASSIGNED {
        v (mV)
58      iglu_trans (mA/cm2)
        ina_trans (mA/cm2)
60      ik_trans (mA/cm2)
        itotal_trans (mA/cm2)
62      iglu_trans_last (mA/cm2)
        ina_trans_last (mA/cm2)
64      ik_trans_last (mA/cm2)
        ina (mA/cm2)
66      ik (mA/cm2)
        iglu (mA/cm2)
68      diam (um)
        total_current (uA/cm2)
70  }

72  STATE {
        glutrans (mol/cm2)
74      glutransGlu (mol/cm2)
        glutransGluNa1 (mol/cm2)
76      glutransGluNa2 (mol/cm2)
        glutransNa (mol/cm2)
78      glutransin (mol/cm2)

80      nai (mM)
        ki (mM)
82      glui (mM)
        nao (mM)
84      ko (mM)
        gluo (mM)
86  }

88  LOCAL volin, volout, surf

90  BREAKPOINT {
        SOLVE scheme1 METHOD sparse
92
        iglu_trans_last = iglu_trans
94      ina_trans_last = ina_trans
        ik_trans_last = ik_trans
96      iglu_trans = total_current*(1e-3)
        ina_trans = -3*total_current*(1e-3)
98      ik_trans = total_current*(1e-3)
        itotal_trans = iglu_trans + ina_trans + ik_trans
100     iglu = iglu_trans
        ina = ina_trans
102     ik = ik_trans
    }
```

```
104    INITIAL {
          LOCAL a1, a2, a3, a4, a5
106       volin = PI*diam*diam/4
          volout = volin*0.2
108       surf = PI*diam

110       iglu = 0
          iglu_trans = 0
112       iglu_trans_last = 0
          ina = 0
114       ina_trans = 0
          ina_trans_last = 0
116       ik = 0
          ik_trans = 0
118       ik_trans_last = 0

120       nai = nain
          nao = naout
122       ki = kin
          ko = kout
124       glui = gluin
          gluo = gluout
126
          a1 = nasrcrate a2=ksrcrate a3=glusrcrate
128       nasrcrate=1e9 ksrcrate = 1e9 glusrcrate = 1e9

130       FROM i=1 TO iter {
             SOLVE scheme1 STEADYSTATE sparse
132       }

134       gluo = 0.5
          nasrcrate = a1 ksrcrate = a2 glusrcrate=a3
136    }

138    KINETIC scheme1 {
          LOCAL x
140       x = F/surf

142       COMPARTMENT volin {nai ki glui}
          COMPARTMENT surf*(1e10) {glutrans glutransGlu
144       glutransGluNa1 glutransGluNa2 glutransNa glutransin}
          COMPARTMENT volout {gluo nao ko}
146
          ~ glutrans + gluo <-> glutransGlu (k12*u(v,
148       -0.1)*surf*(1e10), k21*surf*(1e10)*u(v,0.1))
          ~ glutransGlu + nao <-> glutransGluNa1 (k23*u(v,
150       0.5)*surf*(1e10),k32*surf*(1e10)*u(v,-0.5))
          ~ glutransGluNa1 <-> glutransGluNa2 (k34*u(v,
152       0.4)*surf*(1e10),k43*surf*(1e10)*u(v,-0.4))
          ~ glutransGluNa2 <-> glutransNa + glui (k45*surf*(1e10),
154       k54*surf*(1e10))
          ~ glutransNa <-> glutransin + nai (k56*u(v,
156       0.6)*surf*(1e10),k65*surf*(1e10)*u(v,-0.6))
          ~ glutransin + ki <-> glutrans + ko (k61*surf*(1e10)
```

```
158       *u(v,0.6), k16*u(v,-0.6)*surf*(1e10))

160       total_current = (f_flux - b_flux)*x*(100)

162       CONSERVE glutrans + glutransGlu + glutransGluNa1
          + glutransGluNa2 + glutransNa + glutransin =
164       TotalTrans*surf*(1e10)

166       COMPARTMENT volin {nain kin gluin}
          ~nain <-> nai (nasrcrate*volin, nasrcrate*volin)
168       ~kin <-> ki (ksrcrate*volin, ksrcrate*volin)
          ~gluin <-> glui (glusrcrate*volin, glusrcrate*volin)
170       ~nai << (-(ina-ina_trans_last)/x*(10))
          ~glui << (-(iglu-iglu_trans_last)/x*(10))
172       ~ki << (-(ik-ik_trans_last)/x*(10))

174       COMPARTMENT volout {naout gluout kout}
          ~naout <-> nao (nasrcrate*volout, nasrcrate*volout)
176       ~kout <-> ko (ksrcrate*volout, ksrcrate*volout)
          ~gluout <-> gluo (glusrcrate*volout, glusrcrate*volout)
178       ~nao << ((ina-ina_trans_last)/x*(10))
          ~gluo << ((iglu-iglu_trans_last)/x*(10))
180       ~ko << ((ik-ik_trans_last)/x*(10))
      }
182
      FUNCTION u(x(mV), th) {
184       u = exp((-1)*th*x/(2*(26.7 (mV))))
      }
```